TOPICAL REVIEW

Sintering and microstructure of ice: a review

Jane R Blackford

School of Engineering and Electronics and Centre for Materials Science and Engineering, University of Edinburgh, EH9 3JL, UK

E-mail: jane.blackford@ed.ac.uk

Abstract

Sintering of ice is driven by the thermodynamic requirement to decrease surface energy. The structural morphology of ice in nature has many forms—from snowflakes to glaciers. These forms and their evolution depend critically on the balance between the thermodynamic and kinetic factors involved. Ice is a crystalline material so scientific understanding and approaches from more conventional materials can be applied to ice. The early models of solid state ice sintering are based on power law models originally developed in metallurgy. For pressure sintering of ice, these are based on work on hot isostatic pressing of metals and ceramics. Recent advances in recognizing the grain boundary groove geometry between sintering ice particles require models that use new approaches in materials science. The newer models of sintering in materials science are beginning to incorporate more realistic processing conditions and microstructural complexity, and so there is much to be gained from applying these to ice in the future. The vapour pressure of ice is high, which causes it to sublime readily. The main mechanism for isothermal sintering of ice particles is by vapour diffusion; however other transport mechanisms certainly contribute. Plastic deformation with power law creep combined with recrystallization become important mechanisms in sintering with external pressure. Modern experimental techniques, low temperature scanning electron microscopy and x-ray tomography, are providing new insights into the evolution of microstructures in ice. Sintering in the presence of a small volume fraction of the liquid phase causes much higher bond growth rates. This may be important in natural snow which contains impurities that form a liquid phase. Knowledge of ice microstructure and sintering is beneficial in understanding mechanical behaviour in ice friction and the stability of snow slopes prone to avalanches.

(Some figures in this article are in colour only in the electronic version)

1. Introduction

Ice is a strange material. Its surface is odd—almost a liquid at temperatures approaching its melting point. The solid form of H_2O is less dense than its liquid; fish should be thankful for that. Ice has an amazingly high vapour pressure (this is why very old ice cream tastes like cardboard). But in other ways ice is similar to more conventional materials like metals and ceramics; it is a crystalline solid, has surfaces, grain boundaries and pores and may contain other elements—in solid solution, as precipitates, in solid or liquid form. Ice has many crystal structures (13 have been identified so far). Virtually all ice in nature (and all ice in this review) is the hexagonal form—ice Ih. A metastable cubic form of ice—ice Ic—has been found in the upper atmosphere,

but this transforms to ice Ih at about $-80\,^\circ$C. Ideas, theories, models and experimental techniques used for other materials can be, and have been, used for ice in its various forms.

Ice in nature exists as snow, hail, firn, glaciers, sea ice (and black ice). It has different densities in these forms. Freshly fallen snow often has a density of 100–200 kg m^{-3}. This corresponds to a porosity of ca 80–90%, so there is more 'space' in fresh snow than there is ice. This space plays an important role in the properties and microstructure of snow and how these develop over time. The space is why you can fall softly on snow; why igloos have stunning insulating properties; why it feels way better to ski on snow than ice; and recent developments indicate that it is a key parameter in snow avalanche formation. While this space remains continuous (permeable to fluid), vapour and water can pass through the structure. This is important for the structural development of snow.

Snow forms as flakes in the air. Snowflakes nucleate heterogeneously—often on dust particles in the air. Their subsequent growth is governed by kinetics rather than equilibrium thermodynamics; they grow by vapour deposition processes at high undercoolings (i.e. at temperatures well below the melting point of ice). Their growth is highly sensitive to subtle variations in temperature and humidity—this is why snowflakes have a myriad of different forms.

Snow on the ground undergoes structural changes. These changes are often classified as those occurring isothermally (termed *equilibrium metamorphism* in snow jargon) and those occurring in a macroscopic temperature gradient (termed *temperature gradient* or *kinetic metamorphism*). Surface energy combined with the local and macroscopic temperature and humidity conditions provides the driving force for structural changes in the snow. Metamorphism is microstructural change and may or may not involve a phase transformation; (a phase transformation will be involved if the atomic transport is via sublimation and condensation, whereas there will be no accompanying phase transformation if the transport mechanism is via solid state diffusion). I will consider temperature gradient metamorphism only briefly in this review despite its practical importance in avalanches and snowpack stability. It is dominated by vapour flow and temperature gradients through the snowpack, and the subject of much current research.

A simple way to visualize the changes that occur to a snowflake under isothermal conditions is to imagine its intricate solid shape—with huge specific surface area. The solid will have its lowest energy configuration as a sphere of ice (this, of course, is an oversimplification as crystallographic effects will likely mean that the ice crystal will form facets. Each crystalline phase of ice has a characteristic Wulff plot that determines its equilibrium shape but this will rarely be reached in practice). Even so, the thermodynamics of the system drives the snowflake towards a spherical shape. Now, there is more than one snowflake on the ground; there will be a collection of rounding ice grains (typically several 100s of micrometres to a few millimetres in diameter). Again there is a driving force to minimize the surface area of the system—of the ice grains—so they themselves coalesce or sinter together. The processes at work here are akin to many processes in sintering in powder metallurgy or ceramics. The overall energy of

the system is moving towards a lower energy state. Next, as grain boundaries have energy, the grain boundary area is reduced (this will happen concurrently with the sintering process). These changes often occur through recrystallization (in a metallurgical sense) and grain growth. A good way to view this is to consider the path a snowflake takes to the base of a Polar ice sheet. The snow on the surface of the ice will be highly porous; its density will increase with depth; near the base of the ice sheet it will be nearly solid ice; and the grain size of the ice at the base is often several centimetres—giving an indication of just how much it has changed since it started as a small blob on the surface. The processes inside an ice sheet are analogous to pressurized sintering or hot isostatic pressing of materials.

But the ice at the base of an ice sheet is not completely solid, and it is not quite pure (as seems to me to be the case with almost all materials—they always contain defects and imperfections which can influence their behaviour—subtly or substantially). There are chemical contaminants, or impurities, which may be gas, liquid or solid; their form/location within the microstructure influences microstructural processes and mechanical properties within the ice. For example there are gas filled bubbles or pores at some grain boundaries, liquid-containing veins between grains, and solid dust particles within the ice. These additional chemical species are likely to influence sintering behaviour.

The high vapour pressure of ice causes it to sublime rapidly. This process is also known as (thermal) *etching*. In common with etching in materials science this process reveals grain boundaries and other microstructural features, e.g. etch pits from preferential sublimation at dislocations. This effect is used to see microstructural features in ice (and it can easily be seen on ice that is frozen in a container in a domestic freezer—over a period of days or weeks the grain structure of the ice is revealed). The geometry of a grain boundary where it emerges at the surface of ice is groove shaped. This has been known since the 1960s (Ketcham and Hobbs 1969), but it is only recently that this geometry has been incorporated into studies of sintering of ice particles.

The grain boundary groove geometry of the bond between two sintering ice particles was recognized by Colbeck (1997). All previous studies of sintering of ice, and many other materials, assumed a concave neck at the interface between the grains. Mullins developed the early work on grain boundary grooving in metals several decades earlier (Mullins 1957). The geometry of the groove depends on the interplay of the interfacial energies; the equilibrium values of grain boundary groove angles are used in determining grain boundary and surface energies. The bond geometry will influence the rate and mechanisms of its formation and the mechanical properties. When the grain boundary groove is liquid filled it is generally termed a dihedral angle; the underlying concepts are the same as those for grain boundary grooves. Dihedral angles are important in liquid phase sintering of materials and the geometry of veins in polycrystalline ice.

There is a vast amount of literature covering the science and engineering of ice and snow. It is scattered through different academic disciplines and journals including physics, glaciology, geophysics, surface science and materials. There

are classic textbooks on the physics of ice by Hobbs (1974) and Petrenko and Whitworth (2002), and recent reviews on the structure and mechanical properties of ice (Schulson 1999), snow mechanics (Shapiro *et al* 1997) and avalanche formation (Schweizer *et al* 2003).

This review will bring together sintering studies of ice; microstructural morphology considering the relationship with surface energies between the solid, liquid and vapour phases of H_2O; inter-particle bond geometry; experimental techniques, particularly the importance of newer techniques, e.g. x-ray microtomography and low temperature scanning electron microscopy, where ideas from materials science can make useful contributions to snow and ice as 'materials'; and the importance of ice sintering and microstructure in determining the mechanical properties of bulk systems, with selected examples, e.g. in adhesion and friction.

2. Sintering basics

Kuczynski and Frenkel developed the first quantitative models for sintering in the 1940s (Kuczynski 1949). Over the following two decades the basis of a theoretical framework was established (Lenel 1948, Kingery and Berg 1955, Coble 1958, 1961, 1965, Kingery 1960). Reviews of sintering with overviews of these earlier works have been given by Exner and Arzt (1996) and German (1996). More recently computer simulations have been used which better incorporate the complexity of the processes with many events occurring simultaneously, and model the processes on different length scales (Pan 2003, Olevsky *et al* 2006, Wakai 2006).

This section gives an overview of the important features of sintering processes; their application to sintering of ice is considered more deeply in subsequent sections.

Definition of sintering. 'Sintering is a thermal treatment for bonding particles into a coherent, predominantly solid structure via mass transport events that often occur on the atomic scale. The bonding leads to improved strength and a lower system energy' (German 1996). (In sintering it is important that there is enough thermal energy in the system to enable mass transport; we often think of ice as 'cold'—having a temperature of $0\,^\circ$C or lower—but for ice a temperature just below $0\,^\circ$C is 'hot', there is considerable thermal energy available for atomic movement).

2.1. Driving force for sintering

The reduction in surface energy of the system provides the main driving force for sintering. The Young–Laplace equation gives the stress or pressure σ associated with a surface $\sigma = 2\gamma/r$ where γ is the surface energy and r is the radius of curvature. For a sphere—the smaller the radius of curvature the higher the associated stress and hence the higher the driving force for increasing the radius of curvature (which is the basis for coarsening or Ostwald ripening). Where there is double curvature in the system the Young–Laplace equation generalizes to $\sigma = \gamma(1/r_1 + 1/r_2)$ where r_1 and r_2 are the two principal radii of curvature. This can be applied to the case of a hollow depression or a raised protrusion on a surface—there is a driving force to smooth out the surface. Similarly for two

spherical particles of equal size joined by a bond the radius of the particle is larger than the concave radius of the bond so there is a driving force to move mass to the concave neck area of the bond. There is also a difference in chemical potential (or vapour pressure) between parts of the system with different radii of curvature—an area with a high radius of curvature has a high chemical potential so there is a driving force for material to move to a region of lower curvature to reduce the overall energy of the system. This is the basis for the Kelvin equation which links surface energy, surface curvature and chemical potential.

The mechanisms for sintering depend on the conditions within the system—whether there is liquid present as well as solid, and whether there is an additional external applied pressure. Sintering can be divided into three classes: solid state (or dry) sintering, sintering with an applied external pressure and liquid phase sintering. These classes lead to different microstructures. The microstructure of a solid state sintered arrangement of ice particles is shown in figure 1; the microstructure of a liquid phase sintered arrangement of solid ice particles with the liquid phase (brine) is shown in figure 2.

The resulting structures clearly depend on the amount of solid, liquid and vapour (or pore space) that are present; the proportions of these phases (along with temperature and pressure) also strongly affect the processes that are involved in the formation of the final microstructures. Figure 3 gives a schematic overview of the rich spectrum of structures that can be obtained for H_2O.

2.2. Solid state (or dry) sintering

2.2.1. Geometry of sintering. The sintering of two spheres (or circles in 2D) gives us a simple starting point to consider the behaviour of the system. Over time the bond between the particles, at the neck, grows. In early models the neck is taken to be concave (of reverse curvature compared with the surface of the adjoining spheres); however in crystalline solids the geometry is groove shaped—the absence of the correct geometry, and the difficulty of incorporating it, in models has been recognized (German 1996). Newer more elaborate models include the grain boundary groove geometry. These models are mentioned in section 4.4.

2.2.2. Transport mechanisms. The sintering of particles can occur by several transport mechanisms (figure 4): volume diffusion, surface diffusion, grain boundary diffusion, plastic flow and evaporation–condensation. Often these mechanisms occur simultaneously, and different ones are dominant at different stages of the sintering process. They can be divided into two classes: surface transport (evaporation–condensation and surface diffusion) and bulk transport (grain boundary diffusion and plastic flow); volume diffusion can occur by both surface and bulk transport mechanisms. The source of matter for bulk transport is from the interior of the compact, while for surface transport the matter comes from the surface. Bulk transport mechanisms lead to shrinkage and the mutual approach of the centres of two particles whereas surface transport mechanisms do not lead to shrinkage.
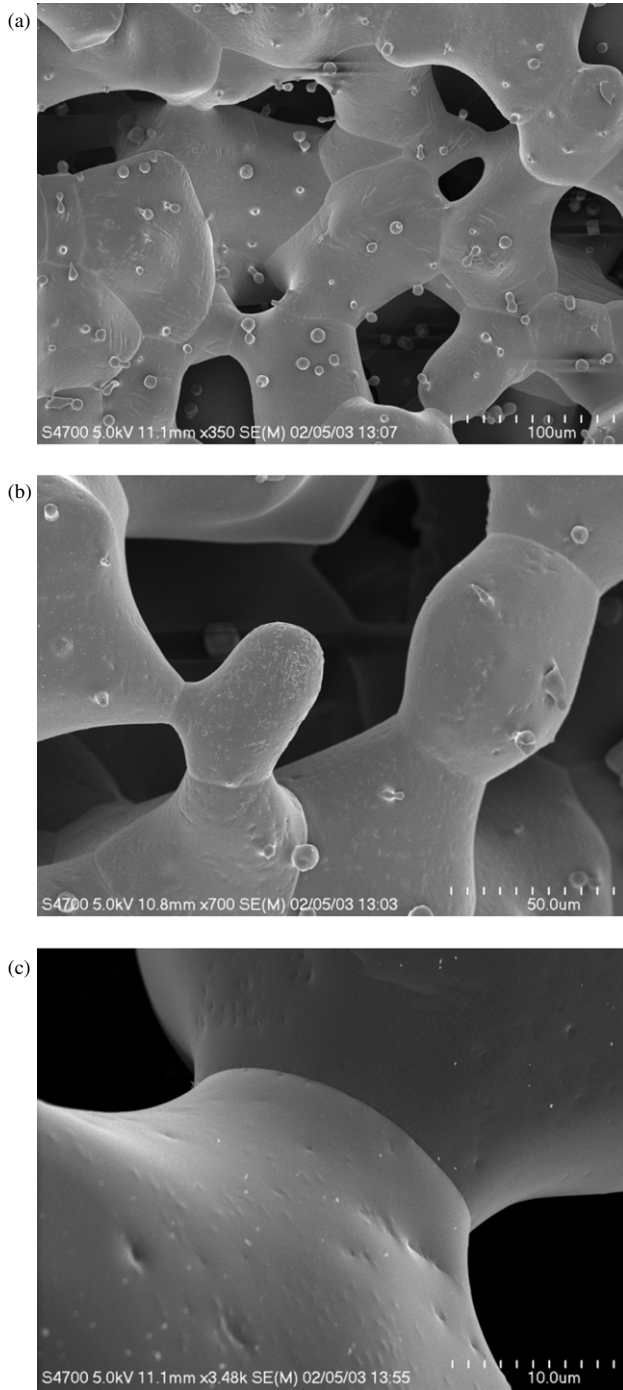
(a)

(b)

(c)

Figure 1. (*a*)–(*c*) Solid state sintering: a series of low temperature SEM images of the microstructure of ice particles, made by spraying water into liquid nitrogen, sintered at −25 °C for 216 h. Grain boundaries can be seen at the necks between the particles; the particles are single crystals.

2.2.3. Stages of sintering, with and without pressure. In the absence of external pressure solid state sintering is driven by the reduction in surface energy and grain boundary energy of the system. The elimination of grain boundary area occurs at more advanced stages and involves coarsening of the microstructure—large particles grow at the expense of smaller ones. Depending on the transport mechanisms—as discussed
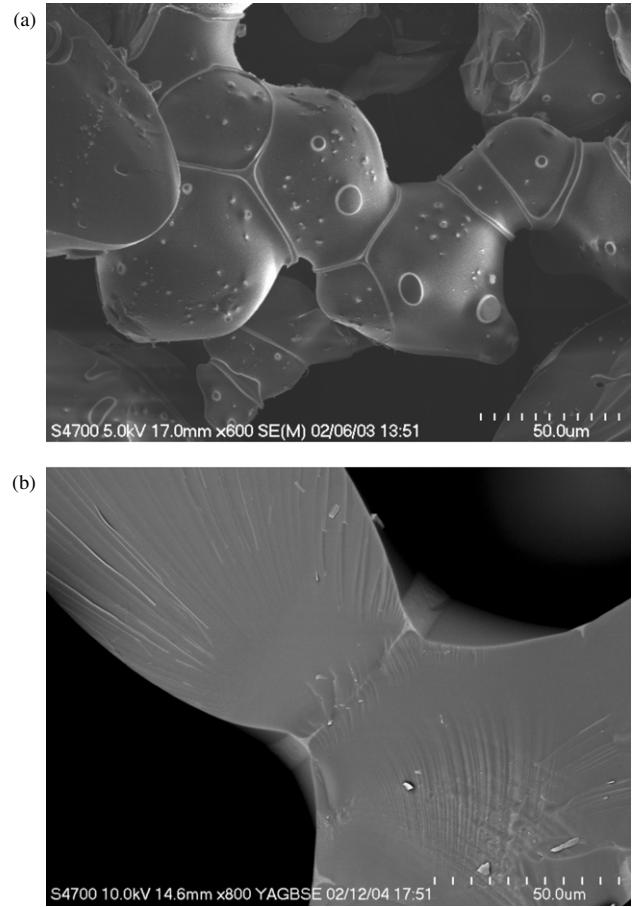
(a)

(b)

Figure 2. Liquid phase sintering: low temperature SEM images of the microstructure of ice particles containing 0.043 M NaCl, sintered. The light shaded web-shaped regions between the solid ice particles, and the smaller circular shaped regions on the surfaces, are rich in NaCl (brine) that was liquid during sintering. (Note: the brine is solid during LTSEM imaging). The liquid brine forms a dihedral angle between neighbouring ice particles. (*a*) Particles as-sintered at −25 °C for 20 h and ice has been removed by etching to show the morphology of the NaCl-containing phase more clearly. The continuous web-shaped ribbons are located at grain boundaries between single crystal ice particles; (*b*) fractured cross section between particles, sintered at −8 °C for 168 h—showing the 2D morphology of the liquid intersecting the grain boundary.

above—a fully dense material can be formed with no external pressure applied to the system.

The driving forces for sintering with an applied external pressure are the surface and grain boundary energies, as with pressureless sintering, and the applied pressure. Material densification will occur with the addition of external pressure to the system. Often the densification behaviour is divided into three stages (although in practice the densification behaviour undergoes a continuous process of evolution): the first is essentially a close packing of the particles in the system (with limited bonding between the particles), the second involves densification until the porosity in the system is closed, the third is closure of the porosity and full densification. Pore space is defined as *open* if it is accessible from the external environment and as *closed* if it is not. In pressure sintering the transport mechanisms are different from pressureless sintering, which results in different final microstructures.
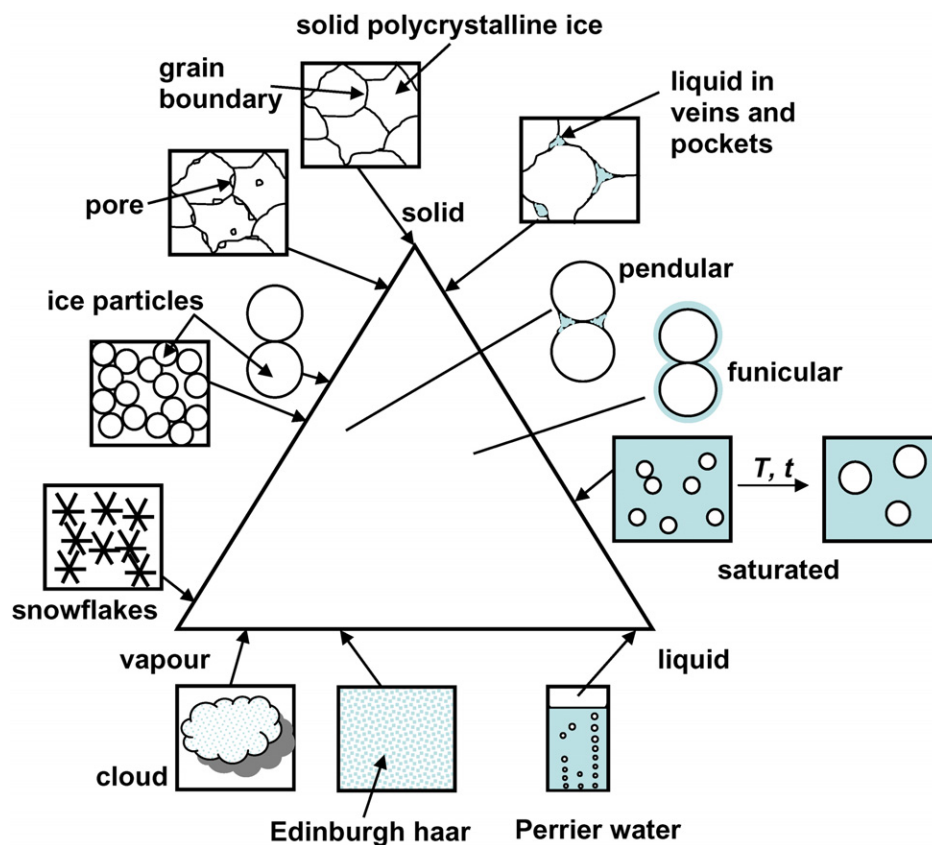
Figure 3. A schematic overview of the spectrum of microstructures that can be obtained for H_2O with varying fractions of solid, liquid and vapour within the structure; for temperatures of $\leqslant 0\,°C$. Although liquid H_2O is not stable below $0\,°C$, the presence of impurities (or deliberately added elements) often results in a depression of the freezing point of H_2O; hence some liquid is present below $0\,°C$. These microstructures are typically transient under specific conditions of formation.
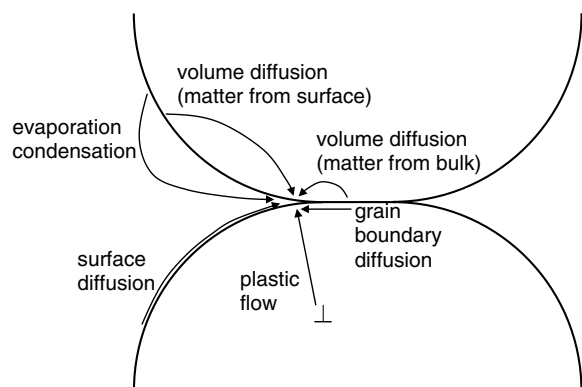

Figure 4. Transport mechanisms in solid state sintering: volume diffusion, surface diffusion, grain boundary diffusion, plastic flow and evaporation–condensation. Often one mechanism is dominant at a particular stage during sintering; however multiple processes contribute.

In commercial systems the aim of sintering is often to achieve a fully dense final product, and by applying a high pressure (along with temperature) more control and reproducibility of the product microstructure is possible, along with shorter cycle times. Hot isostatic pressing (HIPping) of materials is a major industrial technique that enables processing of products (e.g. metal, intermetallic and ceramic powders; and pore closure in castings) that are not possible using other techniques. Fundamental HIPping research, developed for metals and ceramics, has been applied to ice particles sintering under pressure.

2.3. Sintering mechanism maps

The densification behaviour of materials can be depicted using mechanism maps. This approach has been pioneered by Ashby. Mechanism maps are an excellent method for seeing the importance of different transport processes, which lead to densification, how they depend on 'processing' parameters (temperature, time and sometimes pressure) and particle size. Sintering maps, with no applied pressure, provide a useful method for visualizing the results of calculations and experiments of rates of sintering (Ashby 1974, Swinkels and Ashby 1981). Maps of densification behaviour with applied external pressure (often called hot isostatic pressing HIP-maps) have proved to be particularly useful in understanding the contribution from different densification mechanisms and for optimizing materials processing parameters (Arzt *et al* 1983). Pressure sintering maps have been constructed for pressure sintering of ice, as considered in section 4.2.

2.4. Liquid phase sintering

In liquid phase sintering the mass transport occurs predominantly via the liquid phase, by diffusion or convection.

Diffusion in liquid state is much more rapid than solid state diffusion. Convective transport is generally several orders of magnitude faster than diffusive transport—hence rates of liquid phase sintering are typically considerably higher than solid state sintering.

Classically liquid phase sintering is characterized by three stages: the first—liquid flow and particle rearrangement, the second—solution and reprecipitation and the third—solid state sintering/coarsening. Significant structural coarsening (Ostwald ripening) occurs in the second and third stages. Near the start of the liquid phase sintering process (first stage, and between the first and second stages) the liquid penetrates grain boundaries and polycrystalline particles disintegrate; larger particles then grow at the expense of smaller ones.

In commercially relevant liquid phase sintering systems in materials there is a difference in chemical composition of the starting constituents, and ideally the solid phase is highly soluble in the liquid but the liquid has a low solubility in the solid. This ensures liquid is present during the sintering process, which speeds it up and aids densification.

2.5. Equilibrium microstructures and the role of interfacial energies

As discussed at the start of this section, the reduction in surface energy of the system provides the main driving force for sintering—this is true of a system of fine particles with often huge total surface area. However, as we consider the changes the structures go through on their path to equilibrium we see that the interplay of a number of interfacial energies influences the morphology.

The combined effect of the magnitudes of the surface energies between the solid, liquid (if present) and vapour governs the equilibrium morphology of the microstructure (Smith 1948). In a solid state sintered microstructure there are two surface energies that influence the morphology: solid–solid and solid–vapour. The solid–solid surface energy (or grain boundary energy) causes a grain boundary groove to be formed on the surface of a solid in vapour provided there are mechanisms for transport of material for the groove to develop and to form an equilibrium angle (Mullins 1957). This occurs in ice and metals at relatively high homologous temperatures. In a liquid phase sintered microstructure containing vapour there are four surface energies that influence the morphology: solid–solid, solid–liquid, solid–vapour and liquid–vapour. Clearly the system moves to reduce its total energy—so there is competition between the four interfaces, with high energy interfaces being diminished in area. The equilibrium morphology of the bond geometry and the interfacial energy values in solid and liquid state sintering are shown in figure 5. At temperatures at or just below $0\,^{\circ}$C polycrystalline pure H_2O forms a vein system—with liquid water at the grain boundaries in equilibrium with the solid ice. Several experimental and theoretical studies have been reported on this system (Ketcham and Hobbs 1969, Hardy 1977, Walford *et al* 1987, Nye 1989, Walford and Nye 1991, Mader 1992a, 1992b, Dash *et al* 1999, Wettlaufer 1999, Dash *et al* 2006).

2.6. Important physical parameters

In sintering we are often interested in the progression of events during the process—so measures of the system at the start
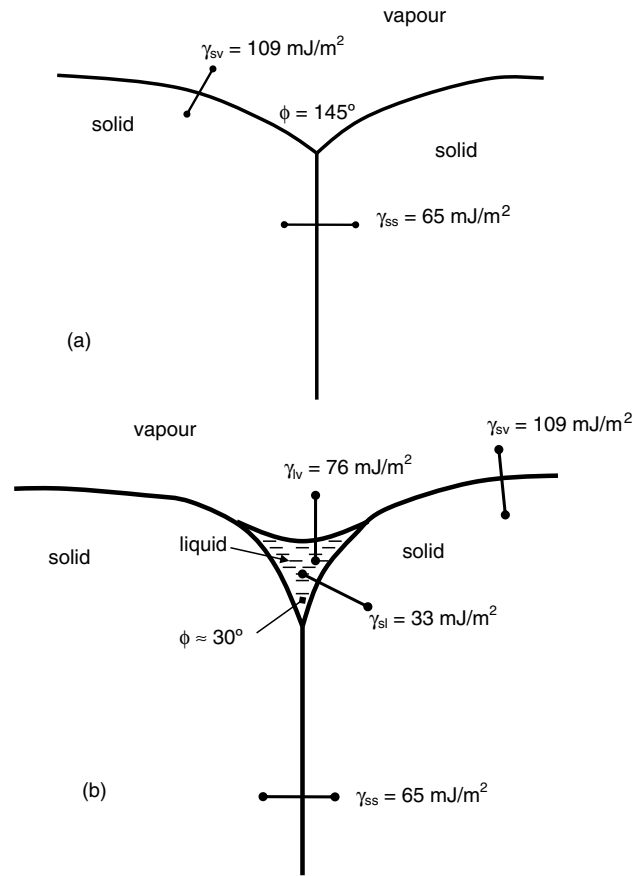

Figure 5. Schematic diagrams for ice to illustrate the geometry of the bonds in (*a*) solid state sintering and (*b*) liquid phase sintering. ϕ is the dihedral angle. A solid state sintered microstructure has two interfacial energies: solid–solid and solid–vapour; and a liquid phase sintered microstructure containing vapour has four interfacial energies: solid–solid, solid–liquid, solid–vapour and liquid–vapour. There is a driving force to reduce the area of high energy interfaces in favour of low energy interfaces. The relative magnitudes of the interfacial energies determine the morphology of the microstructure. Interfacial energies from Ketcham and Hobbs (1969).

and during the process are useful. Processing parameters are time, temperature and pressure and gradients of temperature and pressure. Experimental systems are often designed to produce isothermal and isobaric conditions and these are often assumptions in computer models. In industrially relevant sintering systems gradients of temperature and pressure often lead to unwanted inhomogeneities in the final product. The composition and impurities in the system should be defined.

The starting dimensions of the particles to be sintered are important; in the simplest case we assume a system to comprise uniformly sized spheres, in this case the characteristic measure is the diameter (D). In more complex systems the particle size and shape distribution can be characterized.

The diameter X of the neck between the particles can be measured. This increases during sintering (even if there is no increase in density of the system). A measure of the extent of sintering can be obtained from X/D, the neck size ratio.

The density ρ of the sintered material is a measure of the porosity in the system. Solid volume fraction V_s is defined as $V_s = \rho_c/\rho_t$, where ρ_c is the density of the sintered compact

and ρ_t is the density of the solid material; similarly a volume fraction porosity V_p can be defined as $V_p = 1 - V_s = 1 - \rho_c/\rho_t$. The density also gives a measure of the extent of sintering, assuming the mass transport processes lead to densification. The porosity may be open or closed, and the volume fraction of each can be quantified.

Surface area S decreases during sintering, monitoring the decrease provides a measure of the extent of sintering; quantitatively a dimensionless parameter is used: $\Delta S/S_0$ with ΔS being the change in the surface area ($\Delta S = S_0 - S$) and S_0 is the initial surface area. Surface area can be measured using quantitative stereology techniques or using gas adsorption.

Shrinkage (or swelling) gives an indication of the rates of compaction. This is easily measured by monitoring $\Delta L/L_0$ where ΔL is the change in the length of the compact and L_0 is the initial length. Controlling dimensional changes in sintered products is vital if your aim is to produce near net shape components—so this is important industrially.

Property measurement often gives an indirect indication of sintering. In general, strength increases as sintering progresses. The goal of commercial sintering is to produce materials or products with the required properties—in such a case property measurement may be the most valuable measurement to make (although the pitfall of this approach is that you have no understanding of how these properties arose, which may be a problem if the process stops producing the required material properties). Mechanical property measurement of sintered ice particles, combined with understanding of how these properties arise, is of considerable importance, for example, in understanding how the stability of snow slopes alters over time and influences avalanches, and in understanding the flow of glaciers and ice sheets.

3. Experimental techniques

The microstructure of a material strongly affects its behaviour, so being able to characterize it is important. Techniques provide different information; many of the techniques are complementary, and data from one technique can be validated by using another technique, e.g. if there is an overlap in length scales.

Some structural features in ice and snow can be seen with the naked eye. For example, differences can be seen between hail, freshly fallen snow, old snow—which has transformed to have noticeably larger rounded grains, glacier ice and an ice cube in a gin and tonic. Anyone can see differences in these forms of ice. But someone who knows about materials, particularly ice, will see and interpret features in more depth— the extent of bonding between the grains or snowflakes, the size of the particles, and will sense the density of the ice or snow and bubbles in the ice cube. These bubbles generally form along grain boundaries; so their distribution gives a guide to the grain structure of the ice. The structural features have implications for how the ice behaves. This can be gleaned from a combination of experience and knowledge of: its structure, the way the ice formed and the environmental conditions it has been through, and its properties (can you make a snowball out of it? how deep would you have to plunge an ice axe into it to hold you?. . .).

Looking at the bulk material at a macroscopic level gives a context for your subsequent observations and may help to avoid some pitfalls; materials science and microscopy abound with tales of detailed observations of things that really did not matter, or turned out not to be what the observer thought they were (but equally there are some subtle observations that have turned out to be very important indeed, e.g. fine precipitates or brittle spiky particles in alloys); with techniques having high resolution, small area of sampling (or field of view) and that frequently involve complex sample preparation.

Avalanche practitioners examine snowpack properties and macroscopic structure (e.g. the presence of different layers within the snowpack) in the field to collect data to assess the likelihood of avalanches. Their next stage in increased resolution compared with just looking at the material is achieved with a simple hand lens or magnifying glass and a crystal card (a sheet with mm scale grids). This enables a rapid assessment of crystal size and shape and gives an idea of the bonding between grains. Although the data obtained is approximate it is still valuable when combined with other data: temperature, past, present and future environmental conditions, terrain and experience of the observer. Avalanche practitioners see and understand things; lab based experimentalists, or theoreticians, generally do not.

Although it is possible to elucidate information about ice without any advanced experimental techniques, to probe the structure and properties more deeply a number of techniques create valuable insights. Several structural characterization techniques are covered in this section: light microscopy, low temperature scanning electron microscopy, x-ray tomography and gas adsorption.

Earlier reviews have details of techniques for characterizing the structure of snow, ice and sea ice—these reviews cover a range of length scales from microscopic to macroscopic (Weeks and Ackley 1982, 1986, Shapiro *et al* 1997, Pielmeier and Schneebeli 2003). Weeks and Ackley (1982, 1986) give reviews of the structure and properties of sea ice. Shapiro *et al* (1997) review the state of knowledge in snow mechanics and work on plane section stereology of snow. Pielmeier and Schneebeli (2003) review research on the stratigraphy of snow, including qualitative and quantitative structural characterization techniques and mechanical property testing. They give a good perspective for the historical development of this research from the pre-1900s to the present day, and they point out the limitations of using many of these techniques on natural snow because of the complexity of the structure on different length scales. This review will emphasize recent advances in techniques.

3.1. Light microscopy

Light microscopy is a powerful technique—particularly with the eyes and expertise of a skilled experimentalist. As with all experimental techniques sample preparation is important. Light microscopy using different preparation techniques will allow you to see and quantify different microstructural features. Light microscopy of ice and snow can be carried out either with the microscope in a cold room, or using a cold stage— the latter being more comfortable for the microscopist. It can yield qualitative and quantitative information on solid and

liquid phases. Quantitative microscopy, or stereology, can give grain sizes, shape distribution, crystallographic information, location and distribution of second phases, or impurities.

Light microscopy can be used in reflected, transmitted and polarized light modes. The depth of field for light microscopy is limited (and decreases with increasing magnification), which means that it provides good data for 2D surfaces or cross sections but its use for 3D structures needs to be considered (e.g. by using serial sections; and qualitatively by taking many images to get a feel for what you are actually looking at). Ice is transparent to visible light—this has benefits, e.g. it can be viewed in transmitted light, and drawbacks, e.g. it is difficult to see features on the surface of an ice sample. This can be important when observing samples in reflected light. Reflected light is used for bulk samples and provides an overview of the structure.

Reflected light can be used on porous samples, e.g. snow, which have been impregnated with a material of contrasting colour. The first report of this technique being used for snow was from Bader *et al* (1939). Suitable materials for infiltration have a lower melting point than ice (typically −20 to 0 °C), but freeze at a higher temperature than the imaging temperature, e.g. dimethylphthalate (Perla 1982). 2D images can be obtained by taking plane sections of the infiltrated snow. A good survey of techniques for preparation of plane sections of snow is given by Perla (1982). Samples are prepared by filling the pore space with a supercooled liquid, freezing the infiltrated specimen to create a rigid solid, making a plane surface by cutting and microtoming, and enhancing contrast with further treatments. Perla studied different pore-filling liquids and reviewed earlier studies and noted the high toxicity of some of the chemicals that were used in these earlier studies. Two methods to enhance the contrast of the sections are by rubbing the surface with either (i) water insoluble powders, e.g. carbon, or (ii) water soluble stains, e.g. acid fuchsin; the powders gave sharper outline contrast while the water soluble stains produced more colourful micrographs. This approach has been used for producing a 3D reconstruction of microstructure by taking a series of sections of infiltrated snow at known depths (Good 1987, Brzoska *et al* 1999). This was used for fine and coarse-grained snow and depth hoar reconstruction (Good 1987). These techniques yield information about grain shape and grain boundary position but not about the crystallographic orientation of the grains.

Transmitted light microscopy is made on thin sections (<0.5 mm in thickness). A single grain of ice is birefringent—this allows the relative orientations of crystals (*texture* as it is known in the materials science community or *fabric* in the snow and ice communities) to be determined when a suitable sample is viewed in transmitted polarized light (figure 6). Texture measurement in ice, particularly ice sheets and glaciers, has received a great deal of attention because of its importance for deformation behaviour of the ice; however measurements of textures in snow are less common. A thin section of the ice or snow sample is made and it is viewed between crossed polarizing filters; if a particular grain is aligned such that its *c*-axis is parallel to the direction of transmitted light the grain will appear dark (the extinction position), otherwise it will appear coloured (or grey in black and white images). It is not possible to infer the orientation of a grain from its colour, the sample
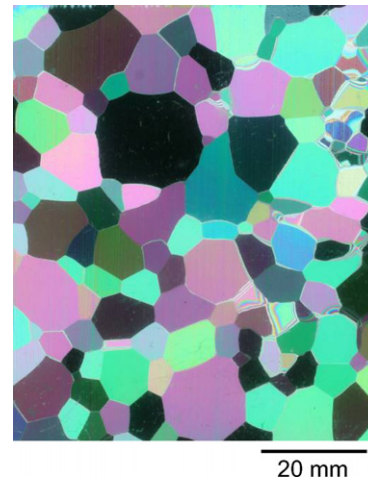

Figure 6. Optical image of a thin section of ice viewed in polarized light, grain boundaries are clearly visible in the structure and the different grain colours are because of the differences in their orientations. From Blackford and Montagnat (2007).

must be tilted on a universal stage to find the extinction position for each grain. A procedure of microtoming the sample from both sides was described for sea ice by Sinha (1977) and for snow, of different microstructures, by Satyawali *et al* (2003). High angle grain boundaries can be seen easily in the thin sections, however thermal etching of grain boundaries is used to identify low angle grain boundaries that do not show up in polarized light because of their low misorientation (Satyawali *et al* 2003).

In recent years significant advances have been made in automatically measuring microstructural parameters and textures of ice samples. These automatic ice fabric analysers provide the orientation of grains from thin sections and generate high quality data rapidly. A thorough review of these techniques has been given by Wilen *et al* (2003). Durand *et al* (2006) have recently proposed an approach for measuring textures and microstructure (including grain size, grain radius, grain size distribution and crystallographic parameters). They have also developed a *Matlab texture toolbox* (which can be downloaded from: http://www.gfy.ku.dk/_www-glac/crystals/micro_main.html). Their work is based within the glaciological community (the authors are in four different institutions in four countries), and it is an excellent example of a collaborative approach to homogenize analysis procedures within a research community. The application of this technique for snow microstructure could be promising.

Kry (1975) has described an optical technique for quantitative measurement of the bonds between rounded snow grains. The method involves producing a thin section from a block of snow infiltrated with a pore-filling material. The section is allowed to sublime—which reveals the grain boundaries between the grains, the boundaries are highlighted with potassium permanganate powder. The technique yields quantitative data on grain size, grain bond size and number density; however it was found that the number of grain bonds per grain could not be determined from the 2D section because of the variation of the shape and size of the grains.

So far we have considered light microscopy for imaging ice and dry snow—that is solid and solid + gas phases. Other

techniques are used for imaging systems containing liquid, e.g. wet snow (solid + liquid + gas) (Brzoska *et al* 1998), and for solid + liquid (Jones and Chadwick 1971, Walford and Nye 1991, Mader 1992a, Williamson *et al* 1999).

Brzoska *et al* (1998) describe a new method for imaging wet snow. Preparing thin sections of wet snow is not possible—as the structural features are lost. They describe a method where the samples are cooled by flash freezing and then sectioned. Analogous techniques are commonly used in metallurgy for imaging semi-solid microstructures. In flash freezing the microstructure of what was the liquid phase in the snow is different from the microstructure of the solid snow grains. A liquid generally contains dissolved gases. If it is allowed to freeze slowly the gases may be expelled, but if it is cooled rapidly the gas is trapped inside the solid and forms bubbles. The flash frozen liquid water contains many finely distributed bubbles. The larger liquid-containing regions can be identified with this technique, which is useful for being able to describe percolation paths in wet snow. However, there was always a discrepancy between the liquid water content of the snow measured by this technique and by calorimetric measurements, and they concluded that flash freezing was not suitable for precisely measuring liquid water contents. They suggest the discrepancy is due to the delayed nucleation of the bubbles on freezing; this was supported by differences seen between sections taken at different depths—which would have undergone different cooling rates.

Arnaud *et al* (1998) describe an excellent optical technique for characterizing the structure of dense snow (firn) and bubbly ice. Polished surfaces are etched and then imaged in coaxial reflected light. This allows imaging of the pore network, grains and grain boundaries. The technique can be used in the field and is rapid; it does not require specimen infiltration or thin sections to be made.

Mader (1992a) made observations and quantitative measurements of the water–vein system in polycrystalline ice. She designed an experimental set up and sample holder to observe and tilt ice samples to enable images of the veins to be taken at different angles. Analysis of the magnified images produced quantitative information on the vein geometry. This technique is an improvement on earlier techniques which measured vein geometry on the sample surface, e.g. by using replicas of the veins (Ketcham and Hobbs 1969).

Walford and Nye (1991) described an optical diffraction method for measuring the dihedral angle of water at a grain boundary in ice. They made observations of water filled lenses which form under pressure at grain boundaries in ice and compared the diffraction patterns with computed diffraction patterns to determine the dihedral angle at the rim of the lens.

Jones and Chadwick (1971) made direct measurements of the geometry in an ice–liquid system (ice–water–NaCl) using a temperature gradient microscope stage. The stage arrangement produced a near vertical ice–liquid interface; for certain grain orientations this created a vertical grain boundary groove, which could be measured and the interfacial energies in the ice–water–NaCl system determined.

Williamson *et al* (1999) describe a method for studying the later stages of coarsening in ice-solute (fructose/water) systems. They measured coarsening kinetics as a function of time and temperature, and made associated observations of

morphology changes in the systems. They used an automated cryo-microscope system consisting of a microscope, a Linkam cryo-stage (temperature control ±0.01 K) heating and cooling modules, suitable for temperature controlled experiments carried out over several days. Image capture with individual frames and video was used. This is an elegant example of making dynamic observations in an *in situ* experiment under thermally controlled conditions.

So far we have considered use of microscopy to image structures of ice and snow; an application where the technique can be useful is in studying snow and ice friction. There has been a lack of microscopic observations on the snow/ice surface after the passage of a slider. Such observations would be beneficial in understanding the frictional processes involved (Colbeck 1992). A report of the use of transparent sliders and optical observations to examine the effects of sliding on snow and ice has been given by Kuroiwa (1977). Differences in the shape and form of the melt layers produced, with glass and PMMA were observed but not explained. A micrograph of the snow surface through the glass slider, after the friction experiment, indicated smoothed snow particles and small entrapped air bubbles in the areas of water films. For the PMMA, streams of meltwater were refrozen as icicles parallel to the direction of sliding, but ice filings were also observed which gathered around the matrix ice particles. This indicates that the abrasion of the ice grains occurred simultaneously with the partial melting of the grains.

Light microscopy in combination with thoughtfully designed experiments can generate a wealth of information and has much potential for the future—but I feel there is a slight danger of its being forgotten or surpassed by newer, fancy techniques—as is the case to some extent in metallurgy and materials science. So use light microscopy wisely along with newer techniques.

3.2. Low temperature scanning electron microscopy

Low temperature scanning electron microscopy (LTSEM) shares with conventional SEM the ability to resolve fine structures two orders of magnitude smaller than in light microscopy; and to view fine structure in the context of large scale morphology. Conventional ambient temperature SEM cannot be used for directly imaging ice or snow. However low temperature LTSEM offers the possibility of imaging cold specimens; a review of the capabilities of ambient and LTSEM has been given by Jeffree and Read (1991). Low temperature scanning electron microscopy has been used for studying ice (Cross 1969, Mulvaney *et al* 1988, Cullen and Baker 2000, 2001, Baker and Cullen 2002, 2003, Barnes *et al* 2002a, 2002b, Iliescu *et al* 2002, Baker *et al* 2003, Barnes *et al* 2003, Obbard *et al* 2003, Barnes and Wolff 2004, Blackford *et al* 2007), snow (Wolff and Reid 1994, Wergin *et al* 1995, 1998, 2002, Rango *et al* 1996a, 1996b, 2000, Wergin *et al* 2002, Dominé *et al* 2003, Erbe *et al* 2003, Legagneux *et al* 2003, Rosenthal *et al* 2007) and ice wear surfaces (Marmo *et al* 2005).

Current state-of-the-art field emission gun (FEG) SEMs have a resolution approaching 1 nm at 15 kV and 2 nm at 1 kV, and 5 nm in the LTSEM mode (cf light microscopy which has a resolution of 1 μm). This offers significant potential for high resolution imaging of the bonds between sintered ice

particles. Another advantage of SEM over optical microscopy for imaging ice is that the ice surface appears opaque, whereas in optical microscopy surface topography is poorly defined because light passes through the surface and contrast can be low. LTSEM is performed in an otherwise conventional SEM fitted with a liquid nitrogen cooled cryo-specimen-preparation unit and a cryo-specimen stage. Techniques for sample preparation for LTSEM ('cryofixation') have been developed extensively for biological specimens (Jeffree and Read 1991, Read and Jeffree 1991). Similar techniques have been used for imaging snowflakes (Wolff and Reid 1994, Wergin *et al* 1995) and metamorphosed snow (Rango *et al* 1996a, 1996b). Wergin *et al* (1998) have made comparisons of images of snow and ice crystals photographed by optical microscopy and LTSEM.

Specimens can be collected in the field and held for long-term storage in a cryostorage system—a liquid nitrogen filled dewar (which can also be used for air transportation). At liquid nitrogen temperature there are no discernible changes in ice morphology over several months. Laboratory experiments on ice particles or snow can be carried out and effectively quenched at any time interval by storing the specimen in a cryostorage system.

In preparing and transferring samples to a LTSEM artefacts are often created from the cryofixation procedures because of contamination with atmospheric water vapour which condenses on the sample. If you are imaging a specimen such as a plant surface, this is less problematic as it is relatively clear what is an artefact and what is 'real' (Jeffree *et al* 1987). However, when imaging ice and snow it is less obvious as ice is contaminated with ice. This effect has been minimized by capping samples during cryofixation then removing the cap for specimen imaging (Barnes *et al* 2002a, 2002b, Marmo *et al* 2005).

Care and experience is needed when interpreting images. This is illustrated by an example of a disputed interpretation of an LTSEM micrograph of snow (Adams *et al* 2001). Their micrograph showed a ridge protruding from the surface of a grain boundary between two snow grains. They assumed the grain boundary ridge was ice and went on to develop a new model for sintering of snow and concluded grain boundary diffusion plays a much more significant role in sintering than previously assumed. The grain boundary diffusivity and width values being about three orders of magnitude higher than previously published values ($D_{gb}\delta$ was calculated to be 2.5×10^3 times higher, where D_{gb} is the grain boundary diffusivity and δ is the grain boundary width). As pointed out by Barnes (2003) their image clearly shows the morphology of two sintered grains with impurities concentrated at the grain boundary between the particles; similar morphologies have been seen in many other systems, as discussed below (and seen in figure 2; although the second phase 'ridge' in this figure is larger in width because of the relatively high salt concentration). However, Adams *et al* did mention that impurities tend to collect at grain boundaries and that these will influence diffusion along the boundaries. The grain boundary structure in ice, how it is affected by impurities and the grain boundary diffusivity are not well known; further research is needed to understand these effects on sintering. So, although Adams *et al* 's interpretation is not correct some of the ideas they discuss would be valuable to follow up.

Additional chemical species are frequently present in natural snow and ice (Legrand and Mayewski 1997, Dominé and Shepson 2002)—detailed study of which is subject to much current research as it is important for understanding and predicting past and future climates, and their presence will influence the mechanical properties of the materials.

The composition, microstructure and location of chemical inhomogeneities, often present as impurities in snow and ice, can be characterized in the LTSEM (Mulvaney *et al* 1988, Cullen and Baker 2000, 2001, Baker and Cullen 2002, Barnes *et al* 2002a, 2002b, Iliescu *et al* 2002, Baker *et al* 2003, Barnes *et al* 2003, Barnes and Wolff 2004, Blackford *et al* 2007, Rosenthal *et al* 2007). Impurities in ice may be present in solid form, e.g. dust particles (Barnes *et al* 2002a, 2002b), or liquid form, e.g. sulphuric acid—at temperatures above $-73\,°C$ which is the temperature of the eutectic in the sulphuric acid–water system (Mulvaney *et al* 1988). Sublimation of superficial ice layers (etching) inside the microscope has been used to gain more detailed information on sub-surface ice structure and on composition, location and morphology of contained impurities. The impurities tend to remain in place on the exposed sample surface and their 3D morphology is revealed as the surrounding ice sublimes. This is a powerful technique to examine microstructure *in situ*, in a way that is not possible with conventional materials.

It is only recently that studies of sintering of snow and ice particles with additional chemical species or impurities using LTSEM have been reported (Barnes 2003, Blackford *et al* 2007, Rosenthal *et al* 2007). Until now most LTSEM studies of snow have concentrated on the snow structure, rather than its evolution, and most studies of impurities in ice have been concerned with Polar ice. Rosenthal *et al* (2007) used an environmental SEM at low temperatures to examine the impurity structures in natural snow. In their study they examined dry and well sintered snow from the Sierra Nevada, California, USA, taken from about 3000 m. They examined the microstructure after 2 days, 5 months and 8 months. They stored the snow at a relatively high temperature of $-20\,°C$ in a sealed container, they observed no discernible change in the structure during the time in storage. Rosenthal *et al* present data that indicate the presence and form of impurities in natural snow: filaments at grain boundaries (although they only observed these in the snow that was stored for 2 days); cobweb like structures, which are networks of impurities covering the grain surface, nodules, and in extreme cases films. Some of these features were observed in the snow after 8 months' storage and after rather aggressive etching (15 min, in vacuum at $-20\,°C$; which caused the ice to disappear so only the impurities remained). EDS analysis of the impurity structures indicated elements that are typical impurities in Sierra snow. They found significant spatial variation in the element concentrations in different locations on the specimens. They observe that the impurities concentrate in the grain boundaries, in regions on the surface and suggest they are also present in the surface pre-melting layer. Over a temperature range where the impurities are liquid (as will be the case often for seasonal snow) they speculate the presence of a liquid phase could modify and control the sintering processes.

The observation of Rosenthal *et al* (2007) that the grain boundary filaments commonly seen in Polar ice were not

visible after storage for 5 months is intriguing. This may point to the complexity of the phase equlibria and kinetic processes in snow and ice containing impurities and the microstructural changes that occurred to their snow during storage. In our studies of a model system of ice particles containing NaCl (Blackford *et al* 2007) (which is a model material for snow sintering with impurities) we observed web like features at grain boundaries that are analogous to grain boundary filaments; these features were however larger in size because of the higher concentration of impurity/salt in the system. The web-like features were liquid brine initially and remained liquid during sintering at $-8\,^{\circ}C$, also these features retained their continuous morphology after sintering for 20 h at $-25\,^{\circ}C$, with the brine forming a pendular ring structure around the grain bonds (figure 2), however sintering for 8 weeks at $-25\,^{\circ}C$ caused the solidified brine (NaCl·2H$_2$O) to break up into discontinuous NaCl-containing precipitates (figure 7). These may be precipitates of NaCl, and further study is required to confirm this; the example is unusual as it is effectively 'reverse coarsening'—as more NaCl-containing-phase/ice boundary is formed over time. Evolution of sintering of ice and snow containing different chemical species is an area for further study.

We have pioneered a technique for studying sintering of ice particles (with or without added impurities/salts) in the LTSEM (Blackford *et al* 2007). We designed a capsule to store the specimens during sintering and to allow them to be transferred and imaged in the LTSEM with minimum contamination from atmospheric water. Ice particles were sintered inside the capsules. The capsules were fitted into a carrier stub before cryofixation. The samples were then cooled in liquid nitrogen and transferred under reduced pressure to the cold stage ($-180\,^{\circ}C$) inside the cryo preparation chamber. The capsules were broken apart (along a glued joint) under vacuum using tools inside the cryo chamber, before imaging in the microscope.

Electron backscatter diffraction (EBSD)—which uses an EBSD detector in an SEM—is now an established technique in materials science and metallurgy. It has proved to be a particularly powerful technique in studying deformation and recrystallization in metals. The crystallographic orientation of small regions of a specimen (down to several micrometres— the size of the interaction volume of the sample with the electron beam) can be characterized. Recently EBSD has been used for ice (Iliescu *et al* 2004, Obbard *et al* 2006), to study recrystallization in Polar ice.

LTSEM enables characterization of ice and snow structural features at high resolution, chemical composition and crystallographic orientation, which makes it a powerful technique especially when used in combination with other techniques.

3.3. X-ray tomography

X-ray microtomography (XMT) provides 3D information of the structure of materials without the need for sectioning. Differences in the x-ray signal depend on the attenuation of the x-rays—so the technique is suitable for materials which have structural features that will provide different x-ray signals, e.g. porous materials and materials that have variations in
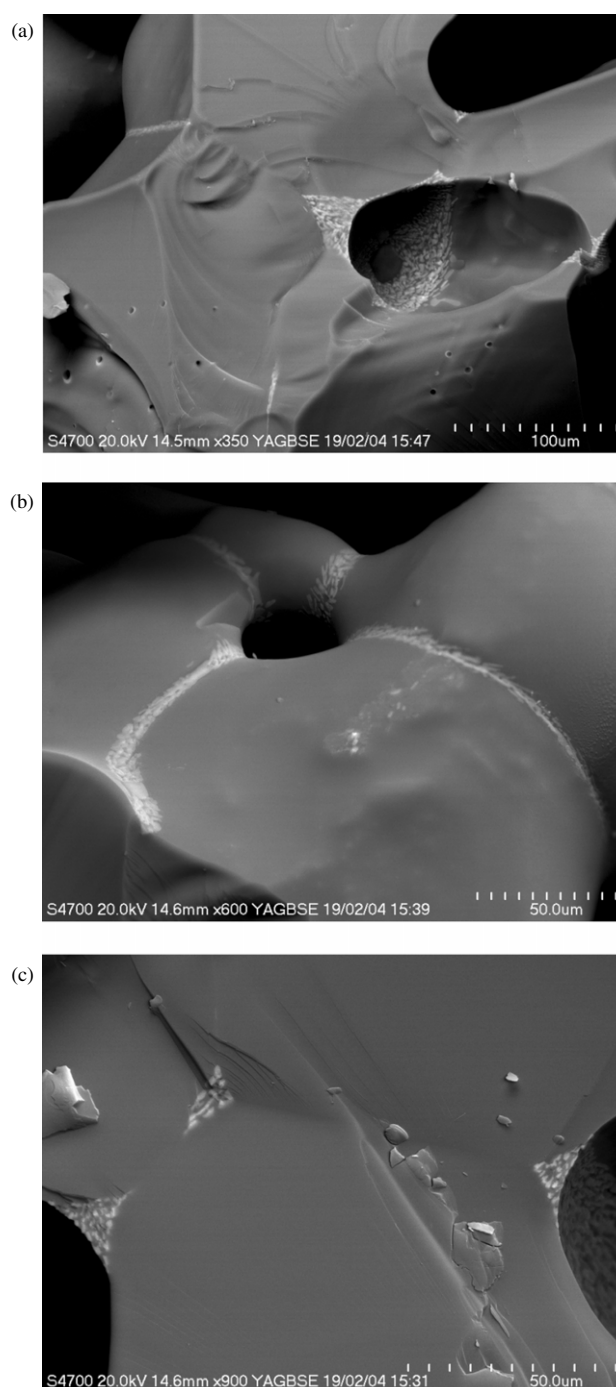

Figure 7. (*a*)–(*c*) Low temperature SEM images of the microstructure of ice particles containing 0.043 M NaCl, sintered at $-25\,^{\circ}C$ for 1344 h. Note that the NaCl-containing phase which was continuous (see figure 2) has broken up into discrete precipitates.

chemical composition which cause different attenuation of the beam. X-ray images of the object are collected at different angles and the resulting images back-projected to reconstruct a three-dimensional view of the object. From this dataset image analysis techniques allow the user to quantify such features as porosity, surface curvature, grain morphology, anisotropy and chemical composition. In materials science typical sample sizes for XMT range from about 10 mm diameter and height to several cm. The spatial resolution depends
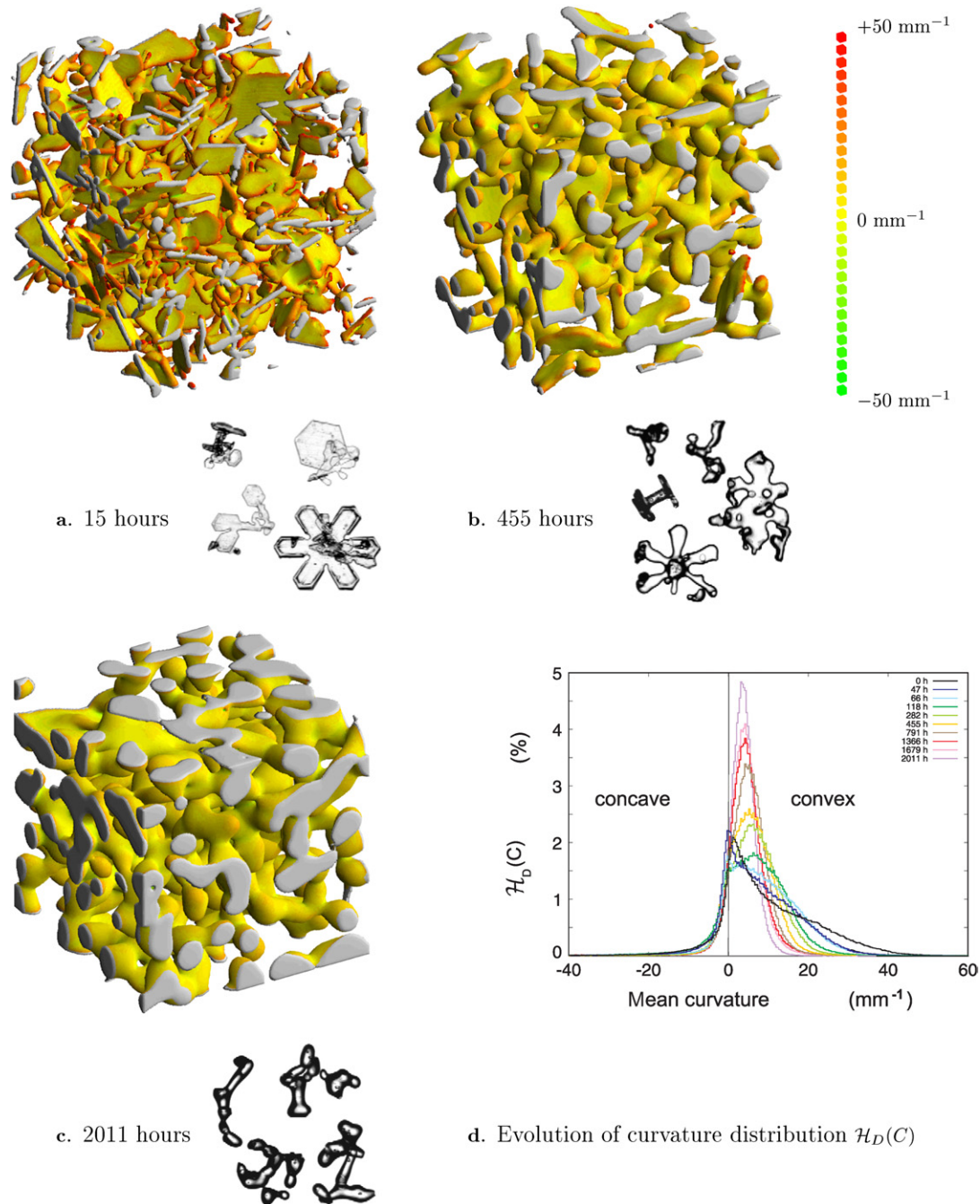
Figure 8. X-ray tomography images of natural sintered snow held at $-2\,°C$ for (*a*) 15 h, (*b*) 455 h, (*c*) 2011 h. (*d*) shows evolution of curvature distribution. Note snow grains coarsen and become more rounded. (Reprinted from Flin *et al* (2004) in the *Annals of Glaciology* with permission of the International Glaciological Society and the authors; image Météo-France—ESRF.)

on the particular instrument. Wildenschild *et al* review XMT systems that have been used in hydrology and provide the following data on resolution: 200–500 μm for medical computer tomography systems, 50–100 μm for industrial systems, 1–50 μm for synchrotron tomography; recent reports give resolutions of 36 μm (Schneebeli and Sokratov 2004) and 40 μm (Freitag *et al* 2004) for snow and firn. However the instrument capabilities are developing rapidly and benchtop XMT devices with resolutions better than 10 μm are becoming relatively common. Figure 8 shows a XMT image of snow.

The typical sample sizes and system resolution make XMT an attractive technique for studying snow (Coleou *et al* 2001, Lundy *et al* 2002, Flin *et al* 2003, 2004, Freitag *et al* 2004, Schneebeli and Sokratov 2004, Kaempfer *et al* 2005), with typical grain sizes in the range of 100 μm to a few mm. XMT is a good technique for studying snow sintering and metamorphism; particularly as it is possible to study the evolution of a single snow sample (without destroying it) over time. Schneebeli and his group at SLF have designed some well thought out experiments to measure the structural changes of snow in a temperature gradient

(Schneebeli and Sokratov 2004) with the aim of quantifying and modelling the snow metamorphism. They use a snow sample in a cell with an imposed temperature gradient inside a tomography unit. Computer models of snow metamorphism are increasingly using XMT data for initial parameters and to verify predictions; quantifying radii of curvature and specific surface area are important for the models (Flin *et al* 2003, 2004, Schneebeli and Sokratov 2004, Kaempfer *et al* 2005, Legagneux and Dominé 2005). XMT is not likely to be useful for studying the location and morphology of impurities in snow because of the low concentrations of impurities and their correspondingly small dimensions (often $<1\,\mu$m) which will not be detected. However, this is where a combination of XMT and LTSEM would be good—as both techniques provide important information and there is an overlap of length scales so the context of the data from the techniques can be understood.

3.4. Gas adsorption

Gas adsorption is used for measurement of specific surface area (SSA) of porous materials, to measure open porosity. In sintering processes SSA generally decreases. This is the case for mechanisms that involve both bulk transport (and lead to shrinkage and densification) and also for surface transport (although there is no densification the structure coarsens and there is a decrease in SSA). In other instances of metamorphism (e.g. temperature gradient metamorphism for snow) SSA changes may be more complex. In atmospheric chemistry measurements of snow SSA are important for quantifying interactions of gases in the atmosphere with the snow cover. A good description of a gas adsorption technique optimized for snow has been given by Legagneux *et al* (2002). They measure the adsorption isotherm of methane at liquid nitrogen temperature (77 K) using a volumetric method, and the isotherm is analysed using the BET (Brunauer–Emmett–Teller) method from which they obtain the surface area of the sample and the net heat of adsorption of methane on ice. They found high SSA values for dendritic snow and that the SSA decreased as the snow aged. They present a method that can be used in the field for estimating SSA by visual examination to an accuracy within 40%.

4. Sintering of ice and snow

Reviews of the sintering of ice and snow have been written by Hobbs (1974), Maeno and Ebinuma (1983) and Colbeck (1997). This section reviews the early work on pressureless sintering of ice spheres and snow, the effect of applied pressure on the system and the depiction of these studies using sintering maps. Ice spheres in an isothermal environment represent the simplest case in sintering of ice. The system becomes more complicated as we consider applied pressure, temperature gradients and microstructural detail (particle geometry and crystallographic effects). We review recent developments in snow, ice and other materials and give some open questions for the future focusing on the details of microstructure, particularly for ice under isothermal conditions.

4.1. Pressureless sintering of ice spheres, experiment and theory—early studies

Experiments on sintering of ice particles have been made by Kingery (1960), Kuroiwa (1961), (1962), Hobbs and Mason (1964), Ramseier and Keeler (1966), Hobbs and Radke (1967) and Jellinek and Ibrahim (1967). A model of sintering of two spheres was first developed for powder metallurgy by Frenkel and Kucynzski (Kuczynski 1949). It is based on a power law equation: $(X/D)^n = Bt/D^m$ where X is the neck diameter, D the particle diameter, t the time, B is a parameter which captures material and geometric constants; B changes with time and extent of sintering. The exponents n and m have different values depending on the dominant mechanism (surface diffusion, $n = 7$, $m = 4$; lattice diffusion, $n = 5$, $m = 3$; vapour transport, $n = 3$, $m = 2$; viscous or plastic flow, $n = 2$, $m = 1$). To find the dominant mechanism in sintering of ice this theory, or modified versions of it, have been applied to ice spheres in several studies (Kingery 1960, Kuroiwa 1961, Hobbs and Mason 1964). These studies made experiments with ice spheres and measured rates of neck growth as a function of time, temperature and radius of the spheres using optical microscopy.

Kingery made ice particles by spraying water into liquid oxygen or liquid nitrogen (Kingery 1960). Particles of 0.1–3 mm radius were produced; experiments were conducted over a temperature range of -2 to $-25\,°$C. Two or more particles were carefully brought together on a microscope slide and their configurational changes measured. At $-2\,°$C the samples were difficult to manipulate and plastic deformation and surface melting tended to occur. Measurements made between the centre points of three or four adjoining spheres over time indicated no shrinkage. This would be consistent with evaporation–condensation (vapour diffusion) or surface diffusion transport mechanisms. From analysis of the neck growth rates as a function of time Kingery concluded that surface diffusion was the dominant mechanism for sintering of ice spheres. This conclusion was later rejected by Hobbs and Mason (1964) as it implied in too large a value for surface diffusion coefficient. This may have been because the ice spheres were not contained within an ice saturated enclosure. (Kingery found $D_o = 10^{18}\,\mathrm{m^2\,s^{-1}}$, where D_o is the pre-exponential factor in the Arhenius expression for D_s the surface diffusion coefficient, and an activation energy of 1.2 eV, which is twice the value for the latent heat of sublimation of ice—so it cannot be correct).

Kuroiwa (1961) also made ice particles by spraying water into liquid oxygen. This resulted in particles of radii 20–500 μm; these were sintered at temperatures between -2 and $-15\,°$C. Again, as Kingery observed, rapid melting and bonding was observed at $-2\,°$C so the results were discounted (but this indicates qualitatively how rapid sintering is with a small volume fraction of liquid phase). Kuroiwa concluded that the dominant transport mechanism was lattice diffusion above $-10\,°$C and surface diffusion below $-10\,°$C. Kuroiwa made experiments in air and with the sample immersed in kerosene. The same values for the exponents in Kuczynski's power law equation were determined for the rates of sintering in both air and kerosene, so Kuroiwa concluded the sintering mechanism was by volume diffusion in both cases. He noted that the neck growth rates in kerosene were very considerably

slower than in air. (In his comparison, the measurements for the sample in kerosene were made at $-3.5\,°C$, while the sample in air was at $-5\,°C$.) So we expect the kinetics in air to be slower than those in kerosene, if the transport mechanism is via volume diffusion, but they are not). Kuroiwa suggested that the slower kinetics in kerosene were because of a decrease in surface energy between the ice surface and the kerosene. However, he appears to have missed a straightforward conclusion that the kinetics were slower in the sample immersed in kerosene because a path in the vapour phase was not available for transport. Hobbs and Mason (1964) rejected Kuroiwa's conclusion that the main sintering mechanism was volume diffusion, as it results in values for bulk diffusion in ice three orders of magnitude higher than those measured by tracer diffusion.

Kuroiwa made some good optical microscopy observations on thin sections from sintered particles. These observations, to some extent, support his conclusion in favour of volume diffusion being an important mechanism. He observed curved grain boundaries at the neck between some particles; such boundaries will have formed by any solid state diffusion mechanism (so volume diffusion is certainly a possibility). Some of his images also show the ice particles, between the necks, to be polycrystalline. We have seen similar microstructures with particles that we have made by a comparable spraying procedure (figure 9). In figure 9 some larger grains can be seen growing at the expense of smaller grains. We have observed that grain growth tends to occur quite rapidly to decrease grain boundary area during sintering treatments. These microstructures evolve so the ice particles between necks tend to become single crystals, as seen in figure 1. This grain growth process will occur by diffusion in the solid state rather than the vapour phase. Kuroiwa also made observations of ice spheres sintering on flat plates of ice (along with doping of the plate or sphere with NH_4F). For pure ice and for the case of the doped ice sphere on a pure plate, a mound appears on the surface of the ice plate; while for the doped plate and pure ice sphere the plate remains flat and material from the plate appears to diffuse into the sphere. He also observes many voids near the interface of the particle and doped plate and suggests a Kirkendall effect due to vacancy diffusion may be occurring. This could be correct, but then we should expect an analogous observation between the doped particle and pure plate, which is not observed. These effects are not fully explained and are worthy of further investigation.

Hobbs and Mason (1964) made a comprehensive study of sintering of single crystal and polycrystalline ice particles, and concluded vapour transport is the dominant mechanism. They used particles of 50–$700\,\mu m$ diameter, and a temperature range of -3 to $-20\,°C$. Their particles were made by using a resonating hypodermic needle device. By varying the resonant frequency they could control the particle size, the particles were allowed to fall through a column cooled by surrounding it with solid carbon dioxide and the particles were collected at the bottom. These particles were polycrystalline. The single crystals were made by nucleating them on silver iodide particles. The single crystals showed slightly lower rates of sintering compared with the polycrystalline particles. They hypothesized this was because the polycrystals retain relatively large areas of high index faces whereas on the single crystals
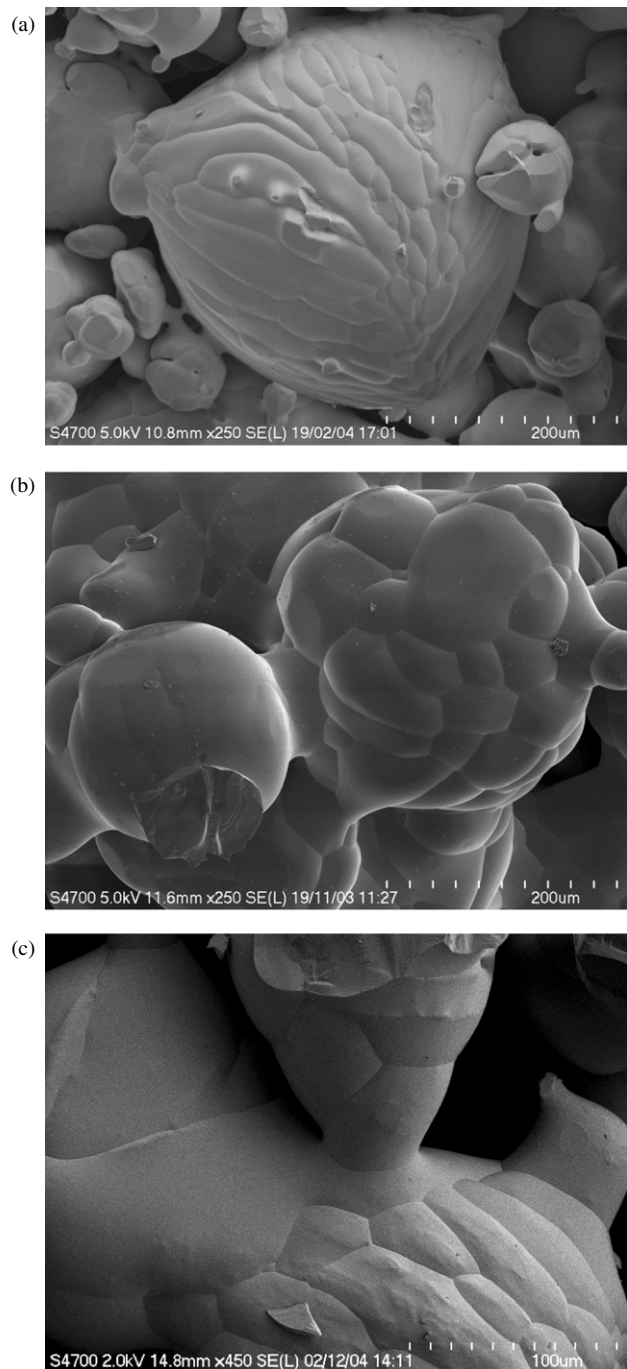

(a)

(b)

(c)

Figure 9. Low temperature SEM images of the microstructure of ice particles made by spraying water into liquid nitrogen and sintered for (*a*) 1 h, $-25\,°C$, (*b*) 48 h, $-7\,°C$, (*c*) 168 h, $-30\,°C$. Note that each ice particle contains many grains, some larger grains are growing at the expense of smaller grains. Longer sintering times lead to more grain growth, many of the ice particles become single crystals and microstructures as in figure 1 evolve.

such high index faces tend to disappear during sublimation. They made a systematic series of experiments altering the surrounding environment, using air that was unsaturated with respect to the ice, hydrogen gas, silicone oil and kerosene. In unsaturated air neck growth was observed for about the first 0.3 h of contact, then it appeared to cease; after about 1 h a reduction in diameter of the particles due to sublimation

was apparent. They suggest that initially the neck growth is controlled by the vapour supply from areas close to the neck that retained ice vapour pressure near saturation (it is also possible that this was because of other mechanisms playing a role in sintering, e.g. the surface transition layer on the ice). They found faster kinetics with a hydrogen gas atmosphere, which is consistent with hydrogen having a higher thermal diffusivity and higher thermal conductivity than air. They studied bond growth between two ice particles that were brought into contact under silicone oil and observed no bond growth; in a similar experiment using kerosene they found limited bond growth—with about a tenth of the rate measured in air, which they attributed to water having a higher solubility in kerosene than silicone oil. However in this experiment it is likely that the oil film would cause the ice particles to remain separate, while the water within the kerosene may promote bonding between the particles.

Hobbs and Mason made measurements on spheres doped with 10^{-2} M solutions of NH_4F, HF and NH_3 and state that in some cases sintering was slightly reduced by these impurities (but they present no results; although this result is inconsistent with their next observation). But they observed much faster kinetics (about 300 times faster) with particles doped with 1% NH_4F and NaCl at $-10\,^{\circ}C$. They explained the more rapid sintering by the presence of a thin layer of liquid on the surface of the spheres. They also noted that when they brought two particles into contact they tended to rotate—this rotation is difficult to explain if there is a uniform liquid film on the particle surface. However, their observation is consistent with our microstructural observations of salt containing ice particles. We have seen that the liquid brine does not form a uniform layer on the particle surface (figure 2), rather it forms discrete regions. When two salt-containing particles are brought into contact, unless the liquid regions happen to line up precisely, it is likely that the particles will rotate because of the capillary forces between the liquid regions.

Hobbs and Mason (1964) modified Kucynzski's model as they considered it was not directly applicable to ice, particularly for vapour transport. The original model assumed the mean free path (MFP) of water molecules at atmospheric pressure in air to be large compared with the neck radius, and the growth rate of the neck to be controlled by both the rate of arrival of molecules and the rate of latent heat of sublimation removal by conduction through air. This is not valid as MFP $= 0.1\,\mu m$ and neck radius $>1\,\mu m$ for $100\,\mu m$ diameter spheres. They used Kelvin's equation as the basis of their calculation to work out the rate of neck growth between two spheres by vapour diffusion: $p = p_o \exp(-2\gamma V_m / rRT)$, where p is the saturated water vapour pressure at an ice surface of radius r at temperature T, p_o is the saturated water vapour pressure over a flat surface, γ is the surface energy of ice, V_m is the ice molar volume and R is the gas constant.

Hobbs and Mason's modified model gave values of $n = 5$ and $m = 3$ for vapour transport; these are the same values as Kucynzski determined for volume diffusion. To distinguish between the mechanisms Hobbs and Mason compared the absolute rates of sintering for the two mechanisms by evaluating the magnitude of B in Kucynzski's power law. Their analysis indicated the neck growth by volume diffusion was about four orders of magnitude slower than by vapour

transport. Hobbs and Mason (1964) found their experimental measurements were about a factor of five lower than their theoretical prediction for vapour transport, but showed the same temperature dependence. The discrepancy between their model and experiments suggests that the model could be improved.

Further evidence for the predominance of vapour transport mechanism was found by Ramseier and Keeler (1966) in their study of compression tests on sintered snow. They allowed snow samples to sinter in air and others were immersed in silicone oil. The rate of strengthening observed in the samples that were immersed under the oil was much lower than those sintered in air. They checked that the silicone oil did not affect the strength of snow compacts, and found it did not, and they found no measurable loss of sample mass to the oil. However, a slight increase in strength was seen for the samples immersed in oil which suggests that some bond growth occurred, which is evidence for other transport mechanisms contributing to sintering in ice.

Hobbs and Radke made a series of isothermal experiments in which they measured the densification of ice spheres (Hobbs and Radke 1967). They state they imposed no external pressure on the ice spheres; however closer examination of their experimental procedures suggests this is not the case. The ice spheres were packed into a balloon and the balloon sealed. They show a photograph of the balloon and the particles can clearly be seen pushing on the surface of the membrane, which suggests that the membrane is imposing a pressure on them. They describe three versions of their experimental apparatus and in one version they are able to impose a pressure on the balloon while it is immersed in an experimental chamber under mercury. They performed a series of experiments at different imposed pressures (0.23, 0.46 and 0.69 m of mercury) and found no difference in the results; but it is likely that the external pressure caused by the balloon membrane was significantly higher than the mercury pressures they applied.

Jellinek and Ibrahim (1967) measured the rate of decrease in surface area in sintering of $1\,\mu m$ diameter ice spheres at -8 to $-35\,^{\circ}C$, using the BET technique. They concluded that the dominant sintering mechanism was by plastic flow, although they used a model developed for sintering of glass beads which is based on viscous flow. As glass is amorphous the viscous flow mechanism is plausible, while for ice it is less likely although the surface of ice is not fully crystalline as mentioned below.

Gubler (1982) measured the tensile force needed to break the bonds between two ice cones after short contact times 1–1000 s, over a temperature range of -0.2 to $-44\,^{\circ}C$, and a contact force range of 0 to 0.1 N. The ice cones were of 20 mm diameter at their base, had a point angle of $45°$ and a tip radius of 0.5 mm. The cones were fixed horizontally in an experimental rig and moved so their tips were slowly brought into contact, held for a period of time, then pulled apart and the tensile force measured. Multiple tests were made with each set of cones, and the cones were allowed to recover for 60 s between tests. The tensile force between the bonds was found to increase rapidly after short contact times, and a maximum was measured at $-5\,^{\circ}C$. A model was devised assuming viscous flow in the ice surface layer, plastic deformation of the cones, freezing of the quasi-liquid layer and
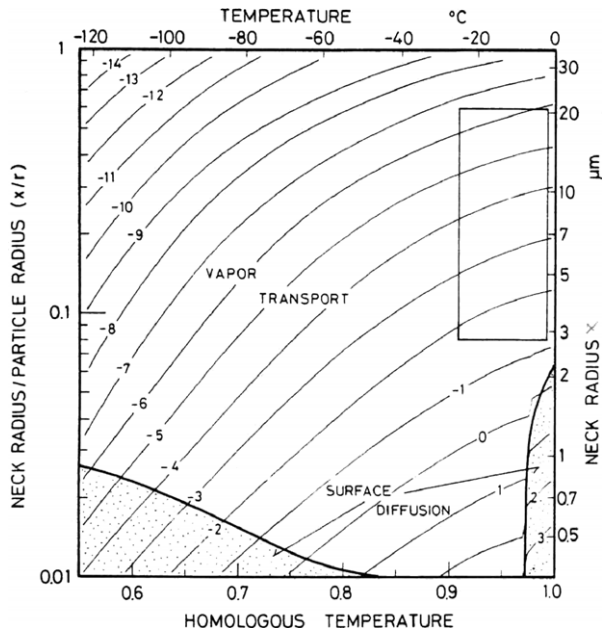
Figure 10. Sintering map for two 35 μm ice particles, with no applied external pressure. The thick lines are the boundaries between the mechanisms where the normalized rates of neck growth are identical from the two mechanisms. The thin lines are contours of constant normalized neck growth rate. The box in the right corner shows the range where experiments have been carried out. (Reprinted with permission from Maeno and Ebinuma (1983). Copyright 1983 American Chemical Society.)

Figure 11. Temperature dependence of the normalized neck growth rates from each transport mechanism for $x/r = 0.01$, where x is the neck radius and r is the particle radius of 35 μm. The numbers indicate the transport mechanisms: 1 = surface diffusion, 2 = lattice diffusion, 3 = vapour transport, 4 = boundary diffusion, 5 = lattice diffusion with matter from grain boundaries. (Reprinted with permission from Maeno and Ebinuma (1983). Copyright 1983 American Chemical Society.)

pressure melting. It should be noted that Gubler's experimental conditions are different from the other studies considered in this section as they involve applied pressure between the ice particles—this will clearly alter the mechanisms of inter particle bonding. In this experiment the microstructure will change during the testing, as the ice cones are repeatedly deformed and fractured—no mention is made of this in the paper. Also there are no comments about precisely where the fracture occurs; it is likely that it is between the cones, but it is possible that material is transferred from one cone to the other.

Maeno and Ebinuma (1983) reassessed data from earlier sintering studies (Kingery 1960, Kuroiwa 1961, 1962, Hobbs and Mason 1964, Ramseier and Keeler 1966, Hobbs and Radke 1967, Jellinek and Ibrahim 1967) and brought it together by plotting sintering maps. They calculated the contribution from six sintering mechanisms using equations from previous studies (Kuczynski 1949, Hobbs and Mason 1964, Johnson 1969, Ashby 1974). They further developed previous studies to include surface diffusion through a surface transition layer on the ice. Their calculations showed surface diffusion in the layer to be important at small neck sizes and at high homologous temperatures, with a rapid increase in rate above −7.5 °C. They also suggest that this effect could be due to viscous flow because of increased mass transport of the water molecules in the layer (Maeno and Ebinuma 1983).

For two 35 μm radius ice spheres they plotted a sintering map to illustrate the regions of dominance for different mechanisms as a function of homologous temperature, neck radius and the ratio of neck radius to particle radius (figure 10). They plotted the contribution from each mechanism as a
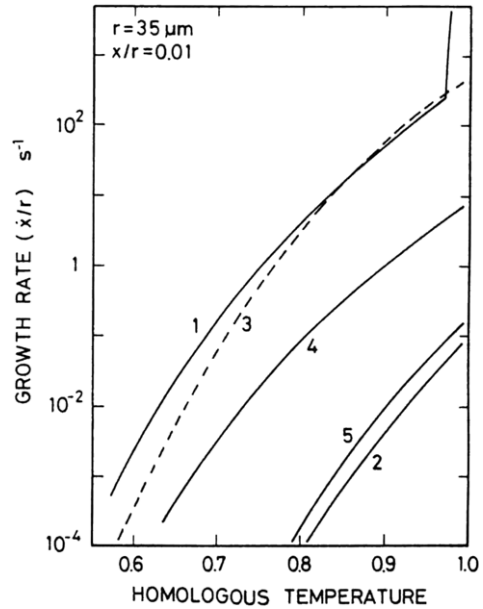
function of temperature (figure 11). The contribution from all mechanisms increases with increasing temperature as would be expected. The predominant mass transport mechanism was vapour diffusion followed by surface diffusion. However other mechanisms they considered (boundary diffusion with the source of matter from the boundary; lattice diffusion with the source of matter from the grain boundary; lattice diffusion with the source of matter from the surface) were found to give important contributions to the mass transport processes.

Maeno and Ebinuma concluded the dominant mechanism for sintering was by vapour transport under most natural and laboratory conditions. However, they predicted two regions where surface diffusion would dominate; at small neck radii (ca <2 μm) at homologous temperatures corresponding to 0 to −6 °C, and (for neck radii of ca <1 μm) below ∼ −40 °C. They made equivalent calculations for 350 μm radius ice spheres and found similar sintering behaviour except that the region where vapour transport was predicted to dominate was even larger.

Vapour transport is so dominant in ice sintering as ice has an unusually high vapour pressure compared with most materials. Typically materials only have a high vapour pressure above their melting point, e.g. the vapour pressure of these substances is 133.3 Pa (1 mm Hg) at homologous temperatures of 0.94 for ice; 0.64 for CO_2; 1.40 for Cu and 1.67 for Al, so apart from CO_2 and ice the vapour transport is only significant above T_m for the other materials. Also, working on experimental ice mechanics in a cold room it becomes very noticeable just how rapidly ice sublimes, over time, typically hours to days, sharp edges become rounded, grain boundaries appear on surfaces, ice debris from sample

machining disappears—all this is clearly visible with the naked eye.

From the work described in this section the vapour transport mechanism stands out as playing a dominant role in sintering of ice particles under most laboratory conditions. Hobbs and Mason's experimental work (Hobbs and Mason 1964) is thorough and particularly convincing. However, it is certain that other transport mechanisms contribute to sintering. Kuroiwa (1961, 1962) observed curved grain boundaries between sintered ice particles, such grain boundary morphology will have formed by a solid state diffusion mechanism; Kuroiwa attributes the morphology to volume diffusion—which is feasible.

Hobbs contradicts his 1964 paper with Mason, on sintering being by vapour diffusion, in a later paper with Radke (Hobbs and Radke 1967), where he concludes volume diffusion has a significant role in sintering. As discussed above, it seems likely that they neglected the contribution from the additional pressure caused by the experimental set-up using a balloon to encase the ice particles. Interestingly, when Hobbs writes about sintering of ice in his monograph *Ice Physics* (Hobbs 1974), he does not mention this publication with Radke on the significant effect of volume diffusion within that section. However, he does refer to this paper in a later section of his book that deals with densification of snow.

Snow on the ground is known to increase in density, typically of time periods of hours to days. This increase in density cannot occur by vapour diffusion as this transport mechanism does not lead to densification. So, other mechanisms must cause the densification; volume diffusion alone is not rapid enough to cause this effect. It is likely that gravity plays a role in densification.

The surface transition layer on ice is an enormous and currently active topic in ice physics. The effect of the surface transition layer of ice on sintering is not certain. Petrenko states that the understanding and properties of the surface of ice 'is probably the most complex and uncertain topic' in his book on the *Physics of Ice* (Petrenko and Whitworth 2002). Pre-melting phenomena on the surface of materials is well known and observed for many common materials close to their melting temperature. Dash *et al* (1995) have reviewed this phenomenon for ice. In Petrenko's review (1994) on the surface of ice he describes experiments that show the liquid-like surface properties on ice are observed at lower temperatures and higher depths than can be attributed to pre-melting alone.

It seems feasible that the surface transition layer has an effect on sintering of ice at short times with ice particles that are free of impurities (impurities will change the surface). If the surface transition layer is similar on two ice particles that are brought into contact, which seems a reasonable assumption, it could cause them to bond rapidly initially. Then there is a difficult question of what occurs in the surface transition layers as bonding occurs. Much is still to be understood about the surface of ice; it is difficult to investigate experimentally as often the techniques interact with the layer and alter it. At present the form and properties of the surface transition layer are not well known, there is controversy about its thickness and the rate of diffusion within the layer. But it may be important for sintering of ice, and more research is needed to answer this. It is not a simple question.

4.2. Pressure sintering of ice

Pressure sintering of ice spheres is relevant for the transitions that occur in glaciers and ice sheets. This is an important subject in glaciology (Gow 1968, 1975, Alley *et al* 1982, Maeno and Ebinuma 1983, Alley 1987, Wilkinson 1988, Arnaud 2000, Freitag *et al* 2004) and has drawn on work and models on hot pressing, particularly hot isostatic pressing, of metals (Wilkinson and Ashby 1975, Swinkels and Ashby 1981, Arzt 1982, Fischmeister and Arzt 1983, Swinkels 1983). As you travel deeper into an ice sheet the pressure increases because of the over burden pressure from the snow and ice above—under these conditions sintering occurs because of driving forces for surface energy minimization and from the external pressure. For example measurements from a core at Camp Century, Greenland, show that at a depth of 12 m the density is $560 \, \text{kg} \, \text{m}^{-3}$ and the age of the ice is 17 y; 40 m, 66 y, $730 \, \text{kg} \, \text{m}^{-3}$; 65 m, 118 y, $820 \, \text{kg} \, \text{m}^{-3}$; 80 m, 152 y, $860 \, \text{kg} \, \text{m}^{-3}$ (Gow 1968, 1975).

Three main stages of densification have been identified for ice sheets, e.g. (Maeno and Ebinuma 1983, Wilkinson 1988, Arnaud 2000), the rate of densification decreases in each stage as the density increases. Images of the structure during densification are shown in figure 12.

Stage 1 is the densification of snow to firn (up to a density of $0.55 \, \text{g} \, \text{cm}^{-3}$ which corresponds to a relative density of about 0.6) from packing of particles by mechanical destruction and grain boundary sliding (Alley 1987), and necks form between particles by diffusion and plastic flow because of the overburden pressure of snow. This packing density corresponds to the maximum dense random packing of granular particles and was first identified for snow by Anderson and Benson (1963); however the material at the end of this stage will have considerable grain boundary area—it will not be a mass of unbonded particles.

Stage 2 is the densification of firn to ice (from $0.55 \, \text{g} \, \text{cm}^{-3}$ to 0.82 to $0.84 \, \text{g} \, \text{cm}^{-3}$, which corresponds to relative densities of 0.6 and 0.88 to 0.91). In this stage the porosity in the system is transformed from interconnected open porosity to closed porosity. This stage proceeds by plastic deformation with power law creep combined with recrystallization. The microstructure consists of large necks between grains with interconnected porosity that is transformed to closed porosity by the end of the stage.

Stage 3 is the densification of bubbly ice (from 0.82 to 0.84, to $0.919 \, \text{g} \, \text{cm}^{-3}$—the density of pore free ice at $-25\,^\circ\text{C}$. All the porosity is closed. Densification proceeds mainly by the same mechanisms as stage 2 but the rate is slowed. In the final stages contributions from other mechanisms are predicted to play a role in densification: lattice diffusion (Maeno and Ebinuma 1983, Wilkinson 1988) and grain boundary diffusion (Maeno and Ebinuma 1983). As the density increases, and the pores shrink, the pressure of gases trapped in the pores rises, which results in an opposing pressure that slows densification.

Maeno and Ebinuma (1983) have plotted pressure sintering maps for stages 2 and 3, using expressions for sintering behaviour based on equations from earlier studies of pressure sintering in metals and ceramics. They superimposed the densification observed from ice core data (at Byrd and
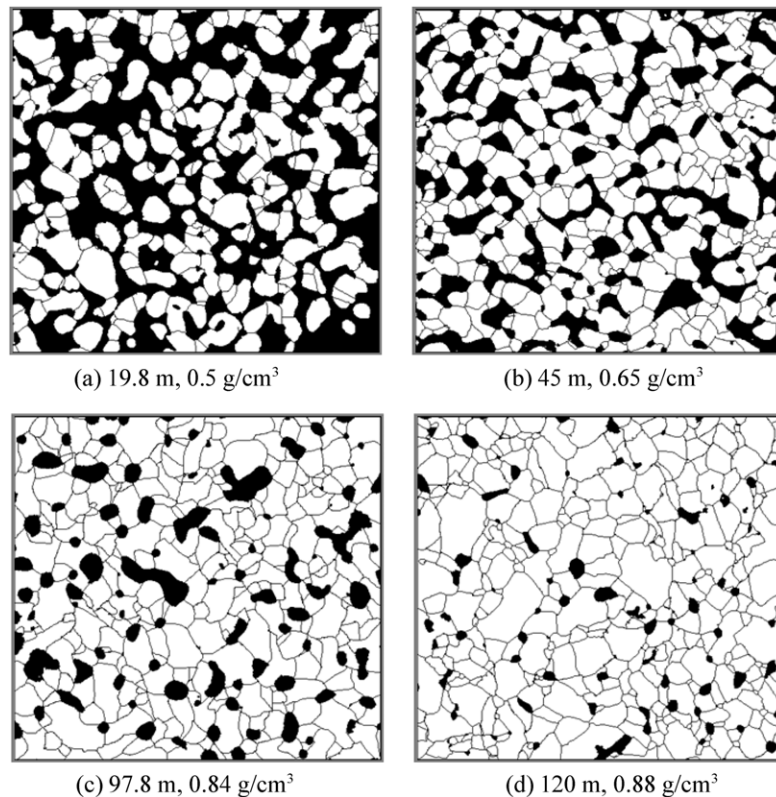
(a) 19.8 m, 0.5 g/cm³

(b) 45 m, 0.65 g/cm³

(c) 97.8 m, 0.84 g/cm³

(d) 120 m, 0.88 g/cm³

Figure 12. Binary images that illustrate the densification stages of snow, firn and ice. Taken from different depths of the Vostok ice core in the Antarctic Polar ice sheet, (*a*) depth 19.8 m, density 500 kg m⁻³ (*b*) 45 m, 650 kg m⁻³ (*c*) 97.8 m, 840 kg m⁻³ (*d*) 120 m, 880 kg m⁻³. (Reprinted with permission of the authors from Arnaud *et al* (2000).)

Mizuho stations) and conclude that the densification of ice cores is predominantly by dislocation creep; however the fields for lattice and grain boundary creep are close by on the sintering map so some contribution to densification from these mechanisms could be expected. In their model Maeno and Ebinuma (1983) approximate the porosity to cylinders between the grains, using an approach based on a model from Wilkinson and Ashby (1975); densification occurs by the reduction in their diameter with a final pinching of the cylinders to form isolated pores by a power law creep mechanism. Recrystallization is not considered in their model.

Recent studies on pressure sintering of ice. Alley (1987) presents an isothermal model for snow and firn densification (up to a relative density of about 0.6) based on grain boundary sliding; the densification mechanism is assumed as the basis of the model—as calculations of densification rates using a combination of power law creep and boundary diffusion and lattice diffusion predicted too low a rate of densification.

Wilkinson (1988) has modelled densification of Polar firn and glacier ice. His model is based on a multimechanism theory of pressure sintering (in a similar approach to that used by Swinkels and Ashby (1981) and Maeno and Ebinuma (1983)). Power law creep was found to be the dominant mechanism between 50% and 98% theoretical density, and lattice diffusion became dominant at low porosities.

Arnaud *et al* (2000) describe a model for the densification of snow, firn and ice. Their model is based on the approaches of Alley (1987) for densification of snow and Arzt (1982) for

densification of the firn and ice by power law creep and the geometrical description for the particle packing. The model shows good agreement with measured densification behaviour of ice cores.

Freitag *et al* (2004) studied the densification of Polar firn using XMT. They measured the densification of snow and firn with depth and found that the particle size of the snow (or ice clusters) caused it to densify at different rates. They state seasonal variations in temperature result in different particle sizes in ice cores—with denser layers deposited in spring to mid-summer and less compressed layers from late summer into autumn. They speculate that the dominant densification mechanism for coarse and fine grained firn operates over different regimes of density, although they do not specify the mechanisms. Alley *et al* also found variations in density of the snow and firn in ice sheets, however they found no correlation with the seasons (Alley *et al* 1982).

Pressure sintering and ice sheets—a huge experimental system for studying material behaviour. In an ice sheet the sintering processes which occur are more complex than the pressureless sintering of two ice particles because of the more complex starting microstructures (snow), temperature and pressure gradients (in addition other chemical species are present in ice sheets which will modify their sintering behaviour). The high temperature gradient is particularly important for the top 2 m where it has a strong effect on the structures that are formed, as considered in section 4.3. The air temperature alters considerably between summer and winter, so there will

be annual cycles in temperature. After ca 10 m ice sheets are generally considered isothermal, and different regions exhibit different mean temperatures, e.g. Vostok $-57\,°C$ and Byrd Station $-28\,°C$; so much of an ice sheet will be isothermal (thousands of metres in many cases). The base of the ice sheets where they are on the ground are at $0\,°C$, which results in a temperature gradient between the cold central part of the sheet and the warmer base. In deeper regions of ice sheets, corresponding to stages 2 and 3 of densification, recrystallization and grain growth become important mechanisms for structural evolution.

However, having identified this complexity—because of the enormous length and time scales involved (seen from the perspective of a materials scientist) many parts of the system can be considered as isothermal and isobaric. This allows us to study the microstructures which have evolved over many human lifetimes; and with careful thought and parameter selection it is possible to design lab experiments to probe the sintering and deformation behaviour of ice over time scales where we can see the results, ideally in small fractions of human lifetimes.

4.3. Non-isothermal metamorphism of snow

In natural snow the effect of the temperature gradient on the system, and the resulting effects on snow metamorphism, are profound—it leads to complex changes in the snowpack structure, which can cause weak layers that result in avalanches. Also the structural complexity of the changes is enormous—and the subject of much research in snow physics and crystal growth; Libbrecht (2005) has written an elegant review that examines the formation and growth of snow crystals. Theoretical (Colbeck 1983) and experimental studies (Marbouty 1980, Sturm and Benson 1997) of temperature gradient metamorphism have been made. Colbeck's theory of dry snow metamorphism accounts for crystal growth of ice particles because of vapour diffusion between them due to temperature gradients in the snow. These temperature gradients are much larger than the temperature gradients due to vapour pressure differences between particles, or around a single particle, in an isothermal system (Colbeck 1983). Snow metamorphism is subject to substantial modelling efforts because of its importance in avalanches (e.g. Brun *et al* 1992, Lehning *et al* 2002). This is a major area of current interest in snow research, but detailed consideration is beyond the scope of this review. More details can be found in a review of snow avalanche formation by Schweizer *et al* (2003).

4.4. Recent developments in sintering of ice and snow

In this section we first review recent work on development of models for sintering of ice and snow. These models draw on microstructural observations but further observations are necessary to confirm them. Two of these studies are directly concerned with sintering of ice particles (Colbeck 1998, Colbeck 2001), while another deals with a more generalized model for metamorphism under both isothermal and non-isothermal conditions (Miller *et al* 2003). Second we consider studies based on experimental evidence from XMT and LTSEM (Dominé *et al* 2003, Flin *et al* 2003, Legagneux *et al* 2003, Flin *et al* 2004, Legagneux *et al* 2004, Legagneux

and Dominé 2005). These studies consider metamorphism of real snow under isothermal conditions, which is more complex than sintering of near spherical particles. Their primary aim is to quantify the specific surface area (SSA) of the snow and its decrease over time; this provides indirect information about sintering—although they are more concerned with surface area than bonding. Quantifying the SSA of snow and how it changes with time are important for modelling the exchange of reactive gases between the atmosphere and snow on the ground, which is important for modelling past and future climates.

4.4.1. Recent models of ice sintering behaviour. There have been two recent reports on isothermal sintering of two particles (Colbeck 1998, Colbeck 2001). These present new theories for sintering and include a grain boundary groove geometry between the particles.

Earlier reports of sintering of ice particles considered the bond between the particles to be a concave neck; the first model to include a grain boundary groove for ice or snow was given by Colbeck (1998). He describes a theory for bond growth via diffusion of water molecules along the inter-particle boundary due to the stress gradient (i.e. grain boundary diffusion). The theory is based on a model from Zhang and Schneibel (1995) for sintering of 2D grains with a constant dihedral angle. Colbeck extends this to 3D grains and includes a dihedral angle that increases with time. The rate of bond growth is linked directly to the rate of increase in dihedral angle. The bond extends because the dihedral angle is not at its equilibrium value which creates a normal stress along the grain boundary. The grain boundary extends when water molecules diffuse along and out of the boundary. The flux of molecules along the grain boundary (J) due to the stress gradient is given by $J = (\delta D_{gb}/kT)(d\Sigma/dy)$, where δ is the width of the diffusive layer at the grain boundary, D_{gb} is the coefficient of grain boundary diffusion, k is Boltzmann's constant, T is absolute temperature, Σ is the normal stress acting across the grain boundary (the tensile stress is positive) and y is the radial coordinate along the boundary.

Colbeck found predictions of sintering rates compared reasonably well with some previous studies (Kingery 1960, Kuroiwa 1962). His computed result shows that $\sin(\phi/2)$ increases as $t^{0.25}$ at the start of sintering, where ϕ is the dihedral angle, which was the highest exponent value found by Kuroiwa in experimental studies of snow sintering. This suggests the theory predicts too high a dependence on time. Also the prediction of grain size may be too high: with the time needed to reach a particular value of dihedral angle increases as r_0^4 (where r_0 is the initial grain radius); Kuroiwa's data suggest a weaker dependence than r_0^2 while Kingery's data indicate r_0^4. However, the exact values of the predictions rely on values for δ and D_{gb} which for ice are not known with enough certainty to be precise.

This model hinges on dihedral angles increasing with time. Colbeck's light microscopy observations suggest that during sintering of particles the dihedral angle increases from low values to the equilibrium value of $145°$. Measuring the angles in the images he presents indicates fresh dry snow with newly formed bonds has angles of approximately $21°$ and $59°$ (measurements taken from opposite sides of the same bond), while bonds between grains stored for several years at $-4.4\,°C$
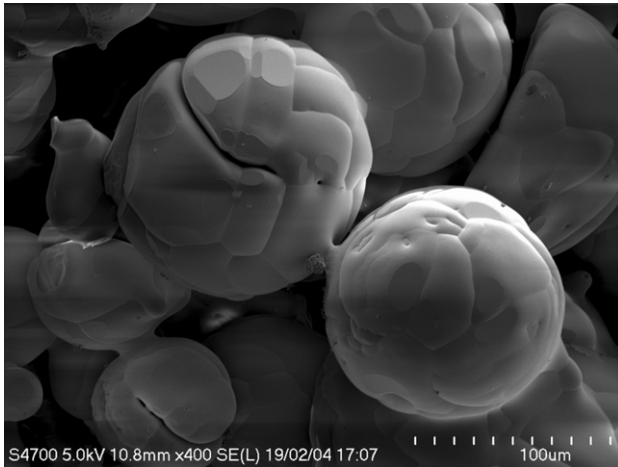
Figure 13. Low temperature SEM image of the grain boundary groove angles of approx 120° between ice particles during early stages of sintering, the dihedral angles in this image range from 118° to 135°; after sintering for 1 h at −8 °C. This value is close to the equilibrium value of 145°, which suggests equilibrium is reached rather quickly even for small neck sizes.

(−24°F) show angles of 143° and 160° (NB it is difficult to measure the angles accurately from the images, but clearly, in the images shown, the dihedral angle is larger in the snow which has been stored for several years). The equilibrium value measured by Ketcham and Hobbs (1969) is 145°. However our LTSEM observations indicate different dihedral angles at short sintering times compared with those observed by Colbeck (1998). We have observed relatively large dihedral angles of approximately 120° between ice particles during early stages of sintering (figure 13, the dihedral angles in this image range from 118° to 135°; and the image was taken after sintering for 1 h at −8 °C). This value is close to the equilibrium value of 145°, which suggests equilibrium is reached rather quickly even for small neck sizes. It is possible that the way our ice particles were made influences their sintering behaviour. The particles were made by spraying distilled water into liquid nitrogen as described by Blackford *et al* (2007). The grain structure of the ice in figure 13 is rather complicated: the ice particles (the large nearly spherical shaped units) comprise many different grains, and many grain boundaries are visible on the surface of the particles. These particles recrystallize with time and tend to become single grains, resulting in microstructures similar to those seen in figure 1. This microstructure is too complex, with recrystallization occurring along with bond growth between particles, to make a definite conclusion about the value of dihedral angle after short sintering times. More systematic observations and measurements are needed to determine how dihedral angles between particles change with time; this is clearly needed to verify Colbeck's model, and to enable comparison with other recent models of sintering. In Colbeck's model the material transport is along the grain boundary, and therefore the model neglects any effect of vapour diffusion, which was found to be the main transport mechanism in earlier studies. However it is important to note that this grain boundary groove geometry can form with any transport mechanisms. Further experiments and modelling are needed to clarify this.

Colbeck (2001) presents a theory for sintering of two unequal sized grains. This theory is generally applicable to any crystalline material. The external surfaces of the grains remain spherical until the smaller grain is consumed. The grain boundary is curved (and is convex with respect to the smaller grain; this is the typical morphology for grain boundaries of grains which are being consumed by grain growth). As in previous models bond growth arises from the gradient of normal stress along the grain boundary.

The theory predicts that as the smaller grain is consumed by the larger one, and the size ratio increases, the stress gradient in the grain boundary decreases and the boundary becomes more curved, which decreases the rate of bonding. The rate of bonding also decreases as the absolute sizes of the particles increase.

At a ratio of 1.57 the surface of the smaller grain is too small to allow it to bond to a third larger grain—so would not easily form a chain of grains. This prediction may be the reason why fresh snow tends to bond slowly to icy surfaces as noted by Colbeck (2001). This is potentially important for avalanche forecasting as if layers do not bond rapidly the avalanche hazard remains higher for longer. In addition to dihedral angle measurements experimental observations of progressive stages sintering of unequal sized particles to examine the movement of the grain boundary are needed to verify whether Colbeck's proposed mechanism is correct.

Miller *et al* (2003) presented a model for metamorphism of dry snow, which considers many particles. The model is applicable for generalized thermal conditions, i.e. isothermal metamorphism and temperature gradient metamorphism. Traditionally studies have separated the metamorphism processes on the basis of the characteristic microstructures produced: rounded grains in an isothermal environment and faceted grains in strong temperature gradients. As Miller *et al* (2003) point out there is a continuum of physical processes contributing to metamorphism, and they develop an approach which unifies the two regimes.

Their model is based on a simple starting microstructure of spherical (or circular) grains with concave necks between the grains, which is similar to the geometry they adopted in an earlier paper on metamorphism of snow (Brown 2001). The model is developed in 2D as a network of grains. The grains can have different sizes. Expressions for heat and mass conservation and phase changes are defined. Mass is allowed to diffuse to or from the ice surface and vertically through the pore space. Heat can flow between the ice grains and to or from the ice surface because of the latent heat exchange from the phase change. They use finite difference methods to solve the non-linear coupled differential equations to give temperatures at nodes in the ice grains and pore space.

Results of their model in isothermal conditions compare well with Hobbs and Mason's (1964) experimental results: the model predicts that sintering rates are rapid at small neck sizes and the rates slow considerably at higher neck sizes; they find a strong dependence on temperature with a factor of eight decrease in bond growth rate from 0 to −20 °C. They find good agreement for bond to grain radius ratio as a function of time at −3 °C; the agreement is less good at −10 °C with the model over-predicting the rate of sintering. They suggest that this poorer fit may be due to the use of a constant diffusion coefficient for water vapour through air, at −10 °C diffusion will be slower which will result in slower sintering.

Under isothermal conditions they assume mass is transported, via the vapour phase, from the large radius of curvature of the grain surface to the neck. When a stronger thermal gradient is imposed on the system the vapour flux leads to mass transport to the neck and also to the grain surface, and to increased vapour transport through the pore network. Miller *et al* (2003) define the transition to kinetic growth as the point when the grain radius ceases to decay. They found kinetic growth is sensitive to bond to grain ratio, grain size and density were important in the onset of this growth form and temperature was relatively unimportant. This approach is promising as, although simple microstructurally, it reproduces empirical trends—it will be useful in predicting metamorphism with alterations in temperature environments which are important practically. Further developments can be envisaged with fewer simplifying assumptions, e.g. encompassing more realistic microstructures.

4.4.2. Recent studies based on new experimental techniques. New experimental work on isothermal sintering and its interpretation is drawing on results from XMT (Flin *et al* 2003, Flin *et al* 2004, Legagneux *et al* 2004, Legagneux and Dominé 2005) and LTSEM (Dominé *et al* 2003, Legagneux *et al* 2003).

Legagneux *et al* (2004) and Legagneux and Dominé (2005) recently studied changes in specific surface area (SSA) of snow during isothermal evolution. Structural changes in snow and SSA are intimately linked with SSA decreasing with time. They carried out a series of experiments at $-15\,°C$ for times up to 141 days. Samples were kept in closed stainless steel containers. Natural snow with different starting morphologies and densities was used. The snow SSA was measured using methane adsorption at 77 K followed by BET treatment of the adsorption isotherm. The technique does not change the snow structure, so it was used to trace the evolution of SSA over time for the same samples.

They found their data fitted well to a logarithmic equation: $SSA = b - a\ln(t + \Delta t)$ where a, b and Δt are adjustable parameters; the equation has no physical basis. b is related to the SSA at the start of the experiment; a is linked to the SSA decay rate; and a and b are linearly linked for a given temperature. They applied grain coarsening theories to the data and concluded isothermal snow metamorphism is governed by similar rules to Ostwald ripening in an initial transient stage, but that a steady state regime is not reached, which means that predicting the rate of decrease of snow specific area using Ostwald ripening theory is difficult.

Legagneux and Dominé (2005) have gone on to develop a mean field model for isothermal snow metamorphism based on transient Ostwald ripening. The snow morphology is represented as a collection of spherical particles. They used simulations to predict values of SSA and distribution of radii of curvature (DRC) for snow from analytical expressions. The values for SSA and DRC were compared with new experimental data from Flin *et al* (2004). The model, compared with the tomographic data, predicts the rate of evolution of particle size distribution well. The fit is shown for data at times between 12 and 2011 h at $-2\,°C$. The initial DRC value is taken as the value after 12 h metamorphism. Although the model predicts particle size distribution well, the calculation

of SSA from DRCs appears to be sensitive probably because of the oversimplification of the geometry of the snow.

Flin *et al* (2004) characterized the microstructural evolution of natural snow held at $-2\,°C$ for up to 2011 h using synchrotron XMT. They calculate the evolution of the curvature distribution with time which can be used in the future for sintering models. Reconstruction of the tomography data shows snow crystal shapes to be clearly visible after 15 h metamorphism; after 445 h the original structure of the snow is still apparent in places, e.g. with crystals with six points, although many of the crystals are coalescing and becoming more rounded; after 2011 h the structure is of rounded bonded grains, with no original six-pointed snow crystals apparent (figure 8). These series of images indicate how complex the changes are that real snow undergoes (especially considering the metamorphism temperature is high, $-2\,°C$, which will result in relatively rapid structural changes) and therefore approximating this structure to an assembly of rounded ice particles is an oversimplification, (although their image at 2011 h approximates to a structure of rounded ice particles, the porosity of 0.7 is still relatively high and corresponds to open porosity).

Flin *et al* (2003) present a 3D model for curvature dependent snow metamorphism. They detail an analytical growth law which depends on the ice curvature and implement a simple numerical model in 3D, which is based on a 2D model first published by Bullard (1997). The local mean curvature of the ice is the main driving force for metamorphism, and the ice is transferred from regions of high mean curvature to low mean curvature; vapour phase diffusion is not considered in the model. They compare their model results with a simulation of simple metamorphism and their XMT data. The model correctly predicts rounding of initial microstructures; the collections of grains on which they tested the model are relatively complex and faceted. At long time scales instabilities appear in the model and strange features develop on the ice surface; also in a collection of grains small particles tend to disappear too slowly—they believe this can be rectified with an improved curvature algorithm.

Legagneux *et al* (2003) studied microstructural changes using LTSEM in snow and made quantitative measurements of SSA under isothermal conditions at -4, -10 and $-15\,°C$ in closed systems. They found crystal rounding was the main process occurring during isothermal metamorphism. However, at $-15\,°C$ they found facets formed on the snow crystals which are not fully explained by current theories of metamorphism.

Dominé *et al* (2003) have presented a detailed study of snow metamorphism using LTSEM. They show many images of natural snow and also carry out isothermal laboratory experiments to investigate the microstructural evolution of snow at -4 and $-15\,°C$. In general their results verify current theories: with sublimating crystals having rounded shapes and crystals growing in temperature gradients having angular and faceted shapes. Isothermal metamorphism at -4 and $-15\,°C$ showed mainly rounded shapes to be formed, which contradicts a hypothesis (Colbeck 1983) that predicts a transition at $-10.5\,°C$ from rounded shapes at higher temperatures to faceted shapes below $-10.5\,°C$. This study gives insights into sintering of ice particles—but deals with a system that has a complex starting geometry—microstructural studies to trace the evolution of structure in simpler systems would be interesting.

4.5. Recent modelling of sintering in materials science

Reviews of modelling of sintering in materials science have recently been published (Pan 2003, Olevsky *et al* 2006, Wakai 2006). These reviews all cover sintering on multiple length scales. Pan's review (2003) brings together significant developments made over the past two decades—and he has neatly classified the models in terms of length scale (atomic, particle and continuum) and discussed how links are being made, and will be made, to join the models over a range of length scales—to produce multiscale models of sintering.

4.5.1. Modelling at the atomic scale. At the atomic scale the sintering of a small cluster of particles can be simulated. Molecular dynamics (MD) is a powerful technique for such simulations. The characteristics of each atomic particle are inputs to the model (composition and crystalline structure) and the output is the trajectory of all the atomic particles. Interpreting the output of the model is critical and this has been subject to much research in materials. In comparison with sintering models on larger length scales MD simulations provide more fundamental insights into the sintering processes as mechanisms, and material properties do not have to be assumed. A major drawback with MD simulations is their extremely small size (up to ca 100 nm) and extremely short time scales (up to 1 ns). Currently, these values are too small to provide useful predictions for sintering of ice particles of the size we have been focusing on in this review. To date a successful application of MD has been in generating diffusion coefficients which can then be used as inputs into sintering models at larger scales. MD is expanding rapidly, and although the simulation of sintering of multiple micron sized particles is not considered to be feasible in the near future (Pan 2003), its impact on simulating materials behaviour will be considerable.

4.5.2. Modelling at the particle scale. In modelling of sintering at the particle scale substantial progress has been made over the last decade or two, but most of this work remains in the realm of materials science and little of it has been applied to sintering of ice. The first modelling at this scale stems from the work of Frenkel and Kuczynski as (detailed in section 4.1), through to the 1970s and 1980s from Ashby and co-workers. All these models have made similar assumptions about the structure of the system, e.g. initially the particles are assumed to be uniformly sized spheres, later transforming to uniformly sized tetrakaidecahedra, with concave necks at the grain boundaries between the particles, and generally one mechanism is considered to be dominant. Recent approaches to modelling at the particle scale have been made with computer simulations using numerical methods. These techniques allow more realistic geometries (particle shape and packing arrangement) to be investigated. Advances have been made in detailed modelling of two, or a few, particles and in modelling systems of several thousand particles, with or without applied external pressure. Clearly the accuracy of the models depends on the quality of the input data, e.g. surface energies, diffusion coefficients for different parts of the system and grain boundary mobility.

Improvements in modelling the solid state sintering of two, or a few (metallic or ceramic), particles with more realistic geometries have been made by Bouvard and McMeeking (1996), Zhang and Schneibel (1995), Svoboda and Riedel (1992) and Pan *et al* (1998). These studies are based on finite difference methods, and all include a grain boundary groove angle between neighbouring grains. Bouvard and McMeeking (1996) simulated the sintering of two spherical particles with and without applied stress using coupled grain boundary and surface diffusion. They found that with no applied stress the results were in good agreement with a simple analytical model, however with an applied stress the particles did not deform as truncated spheres. Zhang and Schneibel (1995) made a 2D numerical study of two particles sintering by surface and grain boundary diffusion and calculate sintering kinetics as a function of dihedral angles and diffusivity parameters. Colbeck applied this model to ice (Colbeck 1998). Svoboda and co-workers have made several detailed modelling studies of sintering at different stages of the process: stage 1 (Svoboda and Riedel 1995), stage 2 (Riedel *et al* 1994, Svoboda *et al* 1994) and stage 3 (Svoboda and Riedel 1992). To model stage 1 of sintering they used three independent techniques—numerical and analytical (approximate and exact). An approximate analytical solution based on a thermodynamic variational principle is likely to be the most practically useful as it allows variations in stress and temperature to be considered. Their approximate analytical solution is based on maximizing the dissipation rate of Gibbs free energy. The expression they used for Gibbs free energy has terms for work done by applied stress, grain boundary energy and surface energy. They found their approximate solution to be accurate for the first stage of sintering but it tended to break down at the second stage because of changes in diffusion conditions. Svoboda *et al* studied stage 2 of sintering with a numerical method; they used a more complex description of the pores, as pillow-shaped gaps with dihedral angles (Svoboda *et al* 1994). They used the results of the microstructural geometry from this study to derive constitutive equations for diffusional densification and creep in stage 2 sintering (Riedel 1994). In studying stage 3 sintering they investigated the slowing of grain boundary migration when a pore is attached to the grain boundary (Svoboda and Riedel 1992) numerically and analytically. They also modelled pore shrinkage together with grain growth and found that 3D pores (closed pores) had a limited retarding effect on migrating boundaries as they were either highly mobile and then moved with the boundary, or had low mobility and separated from the boundary. 2D (cylindrical) pores tended not to separate from the boundary and hence were predicted to slow grain growth when they have low mobility.

To model more than a few particles other techniques are needed. Above we briefly mentioned modelling based on a thermodynamic variational principle (Svoboda and Riedel 1995) or variational calculus. This method has received much attention over the last decade. A set of functions based on the physics and chemistry of the system is used. It is relatively straightforward to add more mechanisms and complexity to the functions. The results of variational calculus are either used directly to obtain approximate solutions for sintering under different conditions (which obviously depend strongly on the physical assumptions that go into the model), e.g. Svoboda and Riedel (1995) and Parhami *et al* (1999), or used as the basis for

finite element (FE) modelling, e.g. (Pan and Cocks 1995, Sun and Suo 1997, Sun *et al* 1997). Using the variational principle for FE is straightforward in 2D but has proved to be much more difficult in 3D. This is because of the huge computing power required for remeshing in 3D compared with 2D.

Another method for modelling multiple particles which is beginning to receive significant attention is the phase field simulation (Kazaryan *et al* 1999, Wang *et al* 2000, Wang 2006). A set of continuum field variables are used to describe the microstructure. The computational power is substantial and supercomputers are needed. This method shows significant promise for realistically simulating the microstructural evolution of hundreds of sintering particles.

Sintering at the particle scale has also been modelled using Monte Carlo (MC) methods (Hassold *et al* 1990, Bordère 2002, Bordère *et al* 2006, Olevsky *et al* 2006). Bordère (2002) and Bordère *et al* (2006) developed a physically based energetic MC model. The later model gave realistic predictions of sintering of crystalline materials in 2D, with or without applied pressure; the results matched the morphologies obtained from analytical solutions. Olevsky *et al* (2006) have used a kinetic MC model to predict sintering stress, bulk viscosity and densification, and have used the values of these parameters as inputs to an FE continuum model. They have successfully used the FE model to predict the dimensional changes in sintering of a zinc oxide ceramic bilayer with two different starting densities in the green as-pressed compact. Olevsky *et al* have carried out a considerable amount of research in continuum modelling of sintering, and more recently on multiscale modelling, which is reviewed in their paper.

4.5.3. Modelling at the macroscopic scale. Although this review is aimed at sintering at the particle level, a brief mention of modelling at larger length scales will be given as it is clearly important for many systems and components. Some of the methods that are used at the particle scale naturally feed into macroscopic models (and with improved computing capabilities it may be possible to use them at macroscopic scales), and an unambiguous classification of models into particle and macroscopic scales is not really feasible as there will be some overlap. The main technique for modelling at macroscopic length scales is the FE method. FE has been used to model sintering, e.g. (Pan and Cocks 1995, Sun and Suo 1997, Sun *et al* 1997, Olevsky *et al* 2006). In FE models the sintering ensemble of particles are considered as a continuum solid, generally with density and grain size defined and tracked during the modelling. FE predicts the final shape of components. The inputs for FE models are based on a constitutive law for sintering, initial properties of the powder compact (density, particle size, etc), temperature and any applied external forces. A difficulty with FE is in incorporating complexity, e.g. the initial packing density of particles and residual stresses, particle size distribution, the effect of chemical composition or impurities in the system, temperature gradients (most FE models of sintering are isothermal).

4.6. Sintering in snow and ice—modelling and experiments—ideas for the future

There is considerable scope to utilize some of the approaches described above in sintering of ice and snow. More detailed

modelling needs to be combined with new experimental observations—which will be inputs for the models and can be used to test the models. A few specific examples are given below:

4.6.1. Dihedral angle changes between sintering particles over time. We need better measurements of how the dihedral angle changes over time, as identified by Colbeck (2001). This is possible with LTSEM.

4.6.2. Grain boundary shape changes during particle coalescence. For sintering of two different sized particles there are models from materials science (Pan *et al* 1998, Wakai *et al* 2005) and for ice (Colbeck 2001). Pan *et al* assumed a flat grain boundary between the particles; while Colbeck used a curved boundary, which is probably more representative. Wakai *et al* (2005) studied a curved grain boundary between two particles which changed shape during sintering, using a numerical technique (the *Surface Evolver* program). They found different sintering morphologies for different surface and grain boundary mobilities and interfacial energies. Observations of the path of the grain boundary motion between ice particles and the particle shapes are needed to examine these models. In addition this motion is likely to be influenced by relative crystallographic orientation of the grains as well as their size ratio.

4.6.3. Pores and bubble morphology in sintered ice. It is generally assumed that the pores are cylindrically shaped during stage 2 and that they become spherical after close-off at the end of stage 2. These morphologies have been used in the models described in section 4.2. There have not been many reports of detailed experimental observations of pores in the literature. However our observations of the pores in ice, and observations from other crystalline materials, reveal that sometimes they have more complex shapes, typically with angles where the pore surface intersects a grain boundary and facets (figure 14). Rango *et al* (2000) have shown LTSEM images of non-spherical bubbles in ice. Barnes *et al* (2002a, 2002b) present a LTSEM image of a pore on a grain boundary, from a Polar ice core sample, which appears to be pinning the grain boundary; there is a clear angle on each side of the pore coinciding with the intersection with the grain boundary. A difficulty they pointed out when studying bubbles from deep cores in ice sheets is that on removing the core from the ice sheet the pressure is reduced. This drop in pressure may allow gases which are dissolved in the ice to come out of solution and form gas bubbles; also the conditions caused by the core drilling may affect the subsequent microstructure of the samples. Some models have considered sintering of non-spherical pores containing dihedral angles (Beere 1975a, 1975b, Svoboda *et al* 1994, Wakai *et al* 2005, Wakai 2006), but these have not been applied to ice yet.

4.6.4. Asymmetric bonds between particles. Experimental observations of bonds between two ice particles sometimes show the join to be asymmetric with one particle forming a longer neck than the other. This observation was mentioned briefly by Colbeck (1997) and was thought to be because
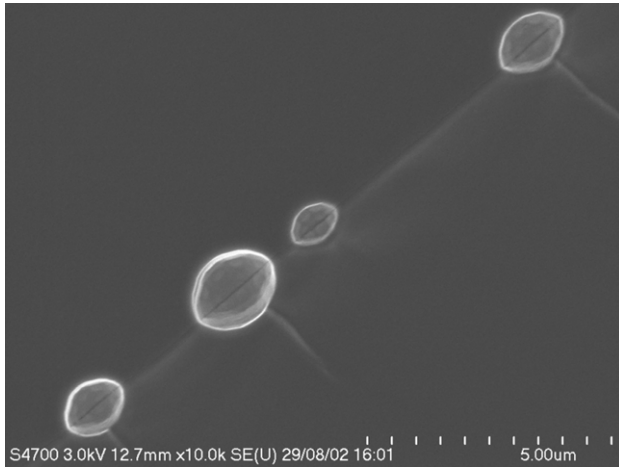
Figure 14. Low temperature SEM image of non-spherical pores along a grain boundary. Note the angles at the edge of the pores where they intersect the grain boundary.

of different crystallographic orientations of the neighbouring grains. Experiments to study this further would be interesting. Also there do not appear to be any sintering models which have considered this effect. However, recently there have been several experimental and modelling studies in materials science that have considered grain boundary grooving with anisotropic surface energies and different crystallographic orientation of the grains (Saylor and Rohrer 1999, Zhang *et al* 2002, Xin and Wong 2003, Zhang *et al* 2004, Zhang and Gladwell 2005, Min and Wong 2006). At specific orientations faceting is also found to occur within the groove to minimize the system energy; Wettlaufer (2001) and Wilen and Dash (1995) have studied these processes extensively on ice. These modelling approaches could be extended to sintering. To achieve this better experimental measurements of bond asymmetry with characterization of crystallographic orientation between the neighbouring grains are needed.

5. Liquid phase sintering

Liquid phase sintering of snow and ice particles has been studied less than sintering in the solid state. In liquid phase sintering there is a spectrum of structures with varying volume fractions of solid, liquid and vapour phases (figure 3). Three structural regimes can be defined on the basis of the location and amount of liquid phases: pendular, funicular and saturated. Vapour is present in the pendular and funicular structures. In the pendular structure the solid phase is continuous and the liquid phase is located around the grain bonds—forming isolated ring-shaped structures known as pendular rings; the liquid phase is not continuous. The funicular structure has a higher liquid volume fraction than the pendular structure and the liquid is continuous throughout. Once all the vapour is removed from the funicular structure it is termed saturated.

Denoth has recently made electromagnetic and hydraulic measurements to determine the structural features associated with liquid water in the snowpack (Denoth 1999, 2003). The electromagnetic measurements used radio and microwave frequencies to directly detect the geometrical location of the water; using these techniques it is possible to identify water

in pendular rings. The hydraulic measurements were made of water percolation or drainage through the snow pack. These measurements are made on bulk snowpacks.

In the pendular regime there are solid, liquid and vapour phases in the structure. There is a relatively low volume fraction of liquid and it forms pendular rings around the bonds between solid particles; the vapour phase is continuous—so transport through this is possible. However, it is likely that transport through the liquid in the pendular rings is the main process for bond growth and structural coarsening (rather than transport though the vapour phase as occurs in solid state sintering of ice) (Colbeck 1997). This is also why coarsening in liquid phase sintering is much more rapid than in solid phase sintering. In this regime a snowpack will gain strength rather rapidly because of a combination of particle rounding, the agglomeration of the particles into clusters, then the growth of solid bonds between the particles. Such processes happen during melt-freeze cycles in snowpacks and lead to substantial increases in strength and stability of the snowpack.

In the funicular regime solid, liquid and vapour phases are present in the structure (the structure is classed as saturated once the vapour disappears—which is essentially an extreme of the funicular regime). These structures are also known as *slush*. The liquid is continuous through the pore space— and transport processes will predominantly occur through the liquid. Percolation or flow of the liquid phase through the structure is easier as the volume fraction of vapour decreases, and with lower solid fractions. This structure results in the funicular regime having profoundly different mechanical properties than the pendular regime, or a porous solid state compact of ice or snow.

This is because the bonds between two solid ice particles are unstable in the funicular regime; while they are stable, or will grow larger, in the pendular and solid state regimes. So, slush has virtually no mechanical strength. Blyth Wright (the director and coordinator for avalanche forecasting in Scotland) has astutely noted that if you make a snowball and can squeeze water out of it, it is a bad sign in terms of slope stability and indicates a high probability of an avalanche (Barton and Wright 2000).

Microstructural changes in liquid phase sintering of ice particles are quite difficult to follow using the experimental techniques considered in section 3. Optical techniques have been used successfully to study coarsening of ice particles in a liquid (Raymond and Tusima 1979, Tusima 1985, Williamson *et al* 1999), and Brzoska *et al* (1998) used a 'flash freezing technique' and optical microscopy and were able to distinguish between the solid ice grains and the liquid from the original sample (see section 3.1). LTSEM and XMT do not naturally lend themselves to studying mixtures of ice and water, as it is very difficult to distinguish the two phases. Environmental SEM may offer more promise in this respect as it should be possible to image wet snow, and potentially its structural evolution *in situ*, though care needs to be taken with precise measurement and control of temperature.

There is a case where the LTSEM may prove very useful. The pendular regime will occur at, or close to, $0\,°C$ for pure H_2O. However, most natural snowpacks are not pure H_2O— they contain impurities (Maupetit and Delmas 1994, Nickus *et al* 1997, Rosenthal *et al* 2007). These impurities can
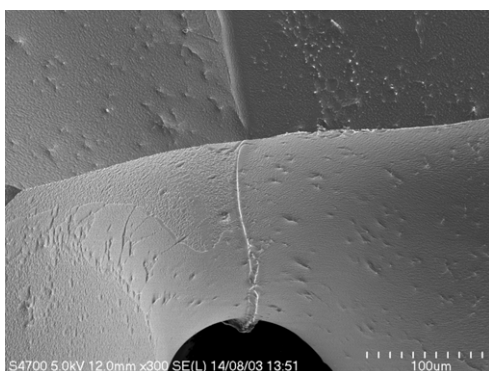
Figure 15. Low temperature SEM image of etched snow from Ben Nevis, Scotland, showing a filament at the grain boundary that is likely to consist of impurities in the snow which have concentrated at the boundary.

cause liquid to be present in the snow at temperatures below $0\,°C$. This means that sintering in snowpacks may be much more strongly influenced by liquid phase sintering (albeit with small volume fractions of liquid) than has previously been realized, which has also been suggested recently by Rosenthal *et al* (2007). Figure 15 shows an etched low temperature SEM micrograph of snow collected from Ben Nevis, Scotland; there is a grain boundary filament on one of the grain boundaries. Our study of sintering of ice particles containing NaCl (Blackford *et al* 2007) is the first study in this direction. Further studies of sintering kinetics and how they depend on impurity content and temperature will be illuminating; ideally these should be combined with measurements of how the mechanical strength develops with sintering.

Liquid phase sintering has been studied considerably in materials science, although the development of theory and models lags behind that of solid state sintering. However some of the techniques and models developed for other materials (Liu *et al* 1999, Liu and German 2001, Lu *et al* 2001, Liu and Fang 2004) could prove useful for snow and ice. A good overview of the principles of sintering in the liquid phase has been given by German (1996); and the state-of-the-art of modelling in liquid phase sintering has been covered in a review by Pan (2003).

6. Mechanical property measurement

In their review of snow mechanics Shapiro *et al* (1997) give a good summary of studies of snow which have investigated microstructure and mechanical properties. One of their key observations is just how much variance there is in the relationships—for example, although strength increases with increasing density there is considerable scatter in the results. This is likely to be because of the microstructural differences in the snow and ice materials that were tested. This is why it is important to know about the microstructure of the material if you want to understand the properties.

The remainder of this section is selective. I highlight recent research that gives good examples of interesting or ingenious work studying the mechanical behaviour of ice and snow which involve sintering.

6.1. Friction on ice and snow and the effect of sintering

Friction on ice is remarkably low because of a lubricating layer of water which forms at the sliding interface because of frictional heating. This was demonstrated neatly by Bowden and Hughes in the 1930s and later by Bowden and Tabor—they made some measurements of friction of skis on snow, near Grindelwald in Switzerland (Bowden and Hughes 1939, Bowden and Tabor 1954). The skis were made from different materials—wood, polymers and brass—and they found that the brass surfaces exhibited the highest friction. This was explained by the principle that frictional heat generated at the interface is conducted into the two sliding materials (i.e. the ski and the snow) and is also used for melting a lubricating layer of water. The brass, of all the ski materials used, had the highest coefficient of thermal conductivity which means it will conduct more heat away from the interface than the other materials, and will therefore retain less heat at the interface for melting a lubricating layer of water. Bowden *et al* made calculations of the effects of frictional heating and of pressure melting on ice friction—these calculations made it clear that, considering the pressure of a ski on snow, pressure melting does not contribute to the low friction on ice, unless the temperature is only a fraction of a degree below zero.

There have been many studies in ice friction—with different sliding materials e.g. polymers and metals—which have technological applications in tyres and winter sports, for example ice skates, bobsleigh and skiing. Ice sliding has also been examined, which is a good system to generate a basic understanding of the mechanisms involved. In ice friction literature it is well known that as the speed of sliding decreases friction increases (Barnes *et al* 1971, Evans *et al* 1976), again this can be linked to the heat generation at the interface—with slower speeds generating less heat and consequently less lubricating water. It is generally considered that the lubricating mechanism dominates at speeds $>0.01\,\mathrm{m\,s^{-1}}$ and that adhesion and plastic deformation, or shear, are dominant below this speed (Barnes *et al* 1971, Tusima 1977). Examination of the ice and its surface after sliding provides direct information on the mechanisms involved; we have developed a technique using the LTSEM to study such ice surfaces (Marmo *et al* 2005). Barnes *et al* observed recrystallization (solid state recrystallization due to plastic deformation, not refreezing of a thin meltwater layer) in the ice after a friction test; similarly recrystallization was observed by Offenbacher *et al* (1973) who showed that it was mainly because of the normal force rather than the frictional force. Recently Maeno and Arakawa (2004) have proposed a modified theory for ice friction at low sliding velocities that incorporates sintering along with adhesion and shear. Their theory of junction growth between asperities because of sintering explains why ice–ice friction continues to increase with decreasing velocity from 10^{-2} to $10^{-7}\,\mathrm{m\,s^{-1}}$.

In some respects friction on ice and on snow differ, this review will not delve into the subtleties of this—but if you are interested in this Colbeck's review of snow friction is a good starting point (Colbeck 1992). However, in some aspects the behaviour of snow and ice are similar—for example, the heat generated from friction which results in the layer of meltwater has important practical significance for both snow and ice. In many cases these effects are well known—such as skating,

skiing, cars skidding on icy or snowy roads. A rather less well-known effect related to friction has recently been observed in snowpacks. It has implications for avalanches, it also involves sintering and will be considered in the next section (Birkeland *et al* 2006).

6.2. Can sintering stop avalanches?

Slab avalanches are generally related to the presence of a weak layer within a snowpack, and the overlying slab fractures along the weak layer (Barton and Wright 2000, Schweizer *et al* 2003). There have been cases where the weak layer has collapsed and the slab moved slightly but a slab avalanche did not occur. The collapse may be accompanied by a 'whumpf' sound—a sound which tends to make people who have some expert knowledge of avalanches in the field feel rather uneasy. Whumpfs have recently been modelled analytically (Heierli and Zaiser 2006, 2007).

In a recent paper avalanche field workers report two cases of accidentally fracturing of a weak layer but in both cases it did not result in a slab avalanche (Birkeland *et al* 2006). This gave opportunities to compare strength measurements of the snowpack before the collapse—of the weak layer itself—and after the collapse. It should be noted that these were single events each observed on one day. The first case was on a North facing slope near Davos in Switzerland, and the second was on a North-East facing slope near West Yellowstone, Montana, in the US; the characteristics of the weak layers were different in the two locations. The weak layer in the Davos snowpack comprised rounded facets and depth hoar crystals. In West Yellowstone the weak layer consisted of two discernible layers of buried surface hoar, after slope collapse the upper layer collapsed while the lower layer stayed relatively intact. The Swiss team used a rammrutsch test and then estimated shear strength values (Schweizer *et al* 1995) and the American team used a shear frame designed by Jamieson and Johnston (2001) for their strength tests.

The shear strength measurements after collapse showed that initially strength was reduced compared with its pre-collapse value but over time a healing or sintering process occurred and the snowpack became stronger. In both cases measurements were taken over a period of about two hours following the collapse. In the Davos case the snow strength was initially 1100 kPa, after collapse it dropped to 900 kPa and after 2 h it increased to 1100–1500 kPa; while in Montana the initial strength was 900–1400 kPa, it dropped dramatically to 300 kPa after weak layer collapse, after 2 h it had regained some strength 400–600 kPa, and measurements the following day indicated similar strength values as those measured before collapse.

The differences observed in the healing behaviour in these two cases are probably related to the different microstructures of the weak layers and differences in their sintering behaviour. As the authors point out, this behaviour is complex and will be influenced by load on the layers, whether further load is being added because of snow fall or wind blown snow, the characteristics of surrounding layers; as well as temperature, the forces and velocities involved in collapse which will cause friction and may lead to melting and subsequent refreezing (liquid phase sintering). These field measurements support the rationale behind a recent model of slab avalanche release

from Fyffe and Zaiser (2004), which examines the effects of weak layer variability and allows for healing within the weak layer.

6.3. Measurements of microstructural properties using a micro penetrometer

Penetration tests of snow have been extensively used to probe the characteristics of the snowpack, with the aim of identifying layers of differing properties which are of importance in slab avalanches as considered above. Recently Johnson, Pielmeier and Schneebeli have designed and built a high resolution penetrometer for use in the field and in the laboratory and developed its use for characterizing microstructural and mechanical properties of snow (Johnson and Schneebeli 1999, Schneebeli *et al* 1999). The instrument comprises a probe which is driven into the snow at a constant speed between 6 and 20 mm s^{-1}. The probe is a small cone shape of 5 mm diameter at its base with a cone angle of 60°, and it is connected to a force sensor which is connected to a main drive rod 1.7 m long. The force sensor has a resolution of 0.01 N and a range of 0 to 500 N. A signal from the force sensor is taken every 0.004 mm (which is considerably less than the typical grain size in snow). Snow densities in the range 50–500 kg m^{-3} have been tested. Force–distance curves are obtained as the probe is driven into the snow and snow bonds are fractured or pushed aside. Different types of snow will clearly produce different signals from the probe and procedures have been devised to obtain microstructural and micromechanical data from the force–distance signals. Also the high resolution in the length scale of the snowmicropen enables thin weak layers in snowpacks to be detected. These instruments are used frequently by avalanche researchers, and routinely by avalanche forecasters particularly in Switzerland. This type of instrument could be used to measure the evolution of mechanical properties during sintering, but so far there are no reports of such studies.

6.4. Insights into sintering of snow from studies of granular media

D'Anna has used a low-frequency forced torsion pendulum to study the mechanical properties of granular media—sand, glass beads and snow (D'Anna 2000). The torsion pendulum is an oscillating cylindrical probe with a cone-shaped end that penetrates the media under test. The system is tested by dynamic oscillation of the probe, and evaluation of the response of the probe gives a measure of dissipation in the system (quantitatively, values of modulus and loss factor are obtained). The snow used was sieved natural snow and it was allowed to sinter, at −13 °C, for different time periods, 3 to 1000 min, before testing. The tests are carried out over about 30 min with varied applied torque. The interactions within the test system will be complex—it is considered likely that the metallic test probe has snow grains bonded to its surface, particularly on the cone-shaped region. The development of the shear strength of the snow over time was fitted with a power law (cautiously because of the paucity of data), with a time exponent of 0.36, which shows reasonable agreement with Colbeck's (1998) value of 0.25. The reasons for the dissipation, e.g. the evolution of the magnitude of the loss peak, in the system are still to be addressed. It is intriguing that the

probe can detect frictional forces that correspond to sintering times which are much longer than the oscillation time of the probe. At high torque amplitudes the bonds between the probe and the snow are continuously broken—so the time available for sintering should correspond to the oscillation period. They speculate this is because the force from the pendulum is dissipated along chains of grains within the snow, rather than being a localized effect.

7. Concluding remarks

Ice is a crystalline material. In many ways its structure and behaviour are similar to those of many other crystalline materials—it is often polycrystalline, so has grain boundaries, it deforms plastically, and may contain impurities or other chemical species (as alloys always do). In other respects ice is rather different from other, more conventional, materials—it has a high vapour pressure which causes it to sublime readily at temperatures below its melting point, crystallographically it is anisotropic (this has implications for plastic deformation and for the surface energies of different planes—and how stable they are on the ice surface) and its surface transition layer is strange. Despite these differences ideas, experimental techniques and models from metallurgy and materials science have been, and can be, applied to ice. This has been a theme throughout this review: starting with the early work on sintering of metals and ceramics from Kucynzski. This approach was applied to sintering of ice in the 1960s by Kingery, Kuroiwa, Hobbs and Mason. Then in the 1970s and 1980s Ashby and co-workers developed models and mechanism maps of sintering and pressure sintering for hot isostatic pressing of metals and ceramics; they also applied this approach to pressure sintering of ice. Modelling of the densification of Polar ice sheets is based on this approach. More recent sintering studies in materials science, from the 1990s onwards, have begun to incorporate some of the more complex, and realistic, features of sintering behaviour—both from modelling and experimental perspectives, e.g. grain boundary grooves and prediction of sintering based on multiple transport mechanisms. This more recent materials science is starting to be applied to sintering of ice, e.g. Colbeck's work on grain boundary grooves in ice sintering.

Ice particles, or snow, undergo different structural changes under isothermal and non-isothermal, or macroscopic temperature gradient, conditions. This review has focused on isothermal sintering, the structural changes are simpler than those that occur under non-isothermal conditions, but as we have seen complex microstructural features still arise. Structural changes of snow under macroscopic temperature gradients are important practically, as they can result in making snow slopes more unstable and likely to avalanche. These changes are dominated by kinetic processes, whereas under isothermal conditions we will get closer to thermodynamic equilibrium.

Isothermal sintering is driven by the thermodynamic requirement to decrease surface energy. Several experimental studies on sintering of ice particles were made in the 1960s. Hobbs and Mason's study stands out as being careful and systematic and shows convincing evidence for vapour diffusion being the predominant mechanism for sintering (when the

vapour path was blocked by immersing the sample in silicone oil the rate of sintering decreased dramatically). Closer examination of the findings from the other experiments by Kingery and Kuroiwa indicates that their results also support vapour diffusion being the main mechanism, although Kuroiwa shows microstructural evidence that indicates other transport mechanisms are operative.

Hobbs and Mason revised the power law model from Kucynzski to make it more applicable for ice. However their model was based on the geometry of the neck at the bond between the particles having a reverse curvature. This geometry is incorrect. The bond between two ice particles has a grain boundary groove, which is a necessity of thermodynamic equilibrium. It is also misleading to think about sintering as occurring by a single mechanism (although one mechanism will often dominate). The difficult question is how large the contribution from each of the transport mechanisms is. Improved knowledge of the diffusion coefficients for ice and the nature of its surface layer are needed to better answer this. But there is strong evidence that vapour diffusion is the main mechanism for isothermal pressureless sintering of ice. Vapour diffusion does not lead to densification. This means that other transport mechanisms must have a role in densification; for this to occur additional forces must act on the system. In a Polar ice sheet there are high external pressures resulting from the thickness of the ice (typically 3000 m). There will be a pressure gradient through the ice sheet, but even the porous snow structure quite near, but below, the surface will be subject to an applied external pressure because of the snow above. As the ice becomes denser plastic deformation with power law creep combined with recrystallization become significant transport mechanisms.

Modern experimental techniques are opening up possibilities for new observations of ice microstructures. Low temperature scanning electron microscopy and x-ray tomography have resulted in new insights into sintering behaviour. LTSEM has provided fine scale structural information on the grain boundary groove geometry of the bonds between ice particles, and on the presence, chemical nature and location of impurities in natural snow and in more controlled laboratory experiments of doped ice. These impurities can be liquid and may play a significant role in sintering of natural snow; small volume fractions of liquid phase are known to strongly increase sintering kinetics. This effect is not well understood. XMT is proving to be a powerful tool particularly to study structural changes in snow in temperature gradients. Also skilful observations of ice microstructures with light microscopy should not be forgotten. Clever experimental design and combined use of these techniques will generate new insights. There is much scope in the future to apply recent models that are emerging from materials science to sintering in ice. Inspiration for some experiments can be taken from these models.

Knowledge of the microstructure of ice helps us better understand aspects of its mechanical behaviour. As with all materials the mechanical properties of ice and snow depend on its microstructure. Sintering of ice plays a role in friction of ice at low sliding velocities, densification of glaciers, ice sheets and snow—and sometimes in healing of flaws in weak layers in slab avalanche prone slopes.

There is still much to be discovered about ice—it is a rich area for study.

Acknowledgments

I thank Laurent Arnaud, Jean-Bruno Brzoska, Geoff Greenwood, Chris Hall, Joachim Heierli, François Louchet, Maurine Montagnat, Moira Wilson and Michael Zaiser for helpful discussions and contributions. I am particularly grateful to my collaborator Chris Jeffree whose exceptional skill in low temperature SEM enabled us to obtain many of the images in this review.

References

Adams E E, Miller D A and Brown R L 2001 Grain boundary ridge on sintered bonds between ice crystals *J. Appl. Phys.* **90** 5782–5

Alley R B 1987 Firn densification by grain-boundary sliding—a 1st model *J. Physique* **48** 249–56

Alley R B, Bolzan J F and Whillans I M 1982 Polar firn densification and grain growth *Ann. Glaciol.* **3** 7–11

Anderson D L and Benson C S 1963 The densification and diagensis of snow *Ice and Snow: Properties, Processes and Applications* ed W D Kingery (Cambridge, MA: MIT Press) pp 391–411

Arnaud L, Gay M, Barnola J M and Duval P 1998 Imaging of firn and bubbly ice in coaxial reflected light: a new technique for the characterization of these porous media *J. Glaciol.* **44** 326–32

Arnaud L, Gay M, Barnola J-M and Duval P 2000 Physical modeling of the densification of snow/firn and ice in the upper part of Polar ice sheets *Physics of Ice Core Records* ed T Hondoh (Hokkaido, Japan: Hokkaido University Press) pp 263–8

Arzt E 1982 The influence of an increasing particle coordination on the densification of spherical powders *Acta Metall.* **30** 1883–90

Arzt E, Ashby M F and Easterling K E 1983 Practical applications of hot-isostatic pressing diagrams—4 case studies *Metall. Trans. A—Phys. Metall. Mater. Sci.* **14** 211–21

Ashby M F 1974 First report on sintering diagrams *Acta Metall.* **22** 275–89

Bader H, Haefeli R, Bucher E, Neher J, Eckel O and Thams C 1939 Der schnee und seine metamorphose *Beitr. Geol. Schweiz., Ser. Geotech. Hydrol.* **3**

Baker I and Cullen D 2002 The structure and chemistry of 94 m Greenland Ice Sheet Project 2 ice *Ann. Glaciol.* **35** 224–30

Baker I and Cullen D 2003 SEM/EDS observations of impurities in Polar ice: artifacts or not? *J. Glaciol.* **49** 184–90

Baker I *et al* 2003 The microstructural location of impurities in ice *Can. J. Phys.* **81** 1–9

Barnes P, Tabor D and Walker J C F 1971 Friction and creep of polycrystalline ice *Proc. R. Soc. Lond. Ser. A—Math. Phys. Sci.* **324** 127–55

Barnes P R F 2003 Comment on 'Grain boundary ridge on sintered bonds between ice crystals' [*J. Appl. Phys.* **90** 5782 2001] *J. Appl. Phys.* **93** 783–5

Barnes P R F and Wolff E W 2004 Distribution of soluble impurities in cold glacial ice *J. Glaciol.* **50** 311–24

Barnes P R F, Mulvaney R, Robinson K and Wolff E W 2002a Observations of Polar ice from the Holocene and the glacial period using the scanning electron microscope *Ann. Glaciol.* **35** 559–66

Barnes P R F, Mulvaney R, Wolff E W and Robinson K 2002b A technique for the examination of Polar ice using the scanning electron microscope *J. Microsc.* **205** 118–24

Barnes P R F, Wolff E W, Mallard D C and Mader H M 2003 SEM studies of the morphology and chemistry of Polar ice *Microsc. Res. Tech.* **62** 62–9

Barton R and Wright B 2000 *A Chance in a Million?* (Scottish Mountaineering Trust)

Beere W 1975a Second stage sintering kinetics of powder compacts *Acta Metall.* **23** 139–45

Beere W 1975b Unifying theory of stability of penetrating liquid-phases and sintering pores *Acta Metall.* **23** 131–8

Birkeland K W, Kronholm K, Logan S and Schweizer J 2006 Field measurements of sintering after fracture of snowpack weak layers *Geophys. Res. Lett.* **33** L03501

Blackford J R, Jeffree C E, Noake D F J and Marmo B A 2007 Microstructural evolution in sintered ice particles containing NaCl observed by low temperature SEM *Proc. IMechE, Part L: J. Mater. Des. Appl.* **221** 151–6

Blackford J R and Montagnat M 2007 unpublished

Bordère S 2002 Original Monte Carlo methodology devoted to the study of sintering processes *J. Am. Ceram. Soc.* **85** 1845–52

Bordère S, Gendron D and Bernard D 2006 Improvement in the accuracy of calculated interface morphologies within Monte Carlo simulations of sintering processes *Scr. Mater.* **55** 267–70

Bouvard D and McMeeking R M 1996 Deformation of interparticle necks by diffusion-controlled creep *J. Am. Ceram. Soc.* **79** 666–72

Bowden F P and Hughes T P 1939 The mechanism of sliding on ice and snow *Proc. R. Soc. Lond.* A **240** 350–67

Bowden F P and Tabor D 1954 *The Friction and Lubrication of Solids* (Oxford: Oxford University Press)

Brown R L, Satyawali P K, Lehning M and Bartelt P 2001 Modeling the changes in microstructure of snow during metamorphism *Cold Regions Sci. Technol.* **33** 91–101

Brun E, David P, Sudul M and Brunot G 1992 A numerical-model to simulate snow-cover stratigraphy for operational avalanche forecasting *J. Glaciol.* **38** 13–22

Brzoska J B, Coleou C and Lesaffre B 1998 Thin-sectioning of wet snow after flash-freezing *J. Glaciol.* **44** 54–62

Brzoska J B, Lesaffre B, Coleou C, Xu K and Pieritz R A 1999 Computation of 3D curvatures on a wet snow sample *Eur. Phys. J.—Appl. Phys.* **7** 45–57

Bullard J W 1997 Digital-image-based models of two-dimensional microstructural evolution by surface diffusion and vapor transport *J. Appl. Phys.* **81** 159–68

Coble R L 1958 Initial sintering of alumina and hematite *J. Am. Ceram. Soc.* **41** 55–62

Coble R L 1961 Sintering crystalline solids: 1. Intermediate and final state diffusion models *J. Appl. Phys.* **32** 787–92

Coble R L 1965 Intermediate-stage sintering—modification and correction of a lattice-diffusion model *J. Appl. Phys.* **36** 2327–8

Colbeck S C 1983 Theory of metamorphism of dry snow *J. Geophys. Res.—Oceans Atmos.* **88** 5475–82

Colbeck S C 1992 A review of the processes that control snow friction *Report* 92-2, US Army Cold Regions Research and Engineering Laboratory, pp 1–41

Colbeck S C 1997 A review of sintering in seasonal snow *Report* 97-10, US Army Cold Regions Research and Engineering Laboratory, 11 pp

Colbeck S C 1998 Sintering in a dry snow cover *J. Appl. Phys.* **84** 4585–9

Colbeck S C 2001 Sintering of unequal grains *J. Appl. Phys.* **89** 4612–18

Coleou C, Lesaffre B, Brzoska J B, Ludwig W and Boller E 2001 Three-dimensional snow images by x-ray microtomography *Ann. Glaciol.* **32** 75–81

Cross J D 1969 Scanning electron microscopy of evaporating ice *Science* **164** 174–5

Cullen D and Baker I 2000 The chemistry of grain boundaries in Greenland ice *J. Glaciol.* **46** 703–6

Cullen D and Baker I 2001 Observation of impurities in ice *Microsc. Res. Technol.* **55** 198–207

D'Anna G 2000 Mechanical properties of granular media, including snow, investigated by a low-frequency forced torsion pendulum *Phys. Rev.* E **62** 982–92

Dash J G, Fu H Y and Wettlaufer J S 1995 The premelting of ice and its environmental consequences *Rep. Prog. Phys.* **58** 115–67

Dash J G, Hodgkin V A and Wettlaufer J S 1999 Dynamics of faceted grain boundary grooves *J. Stat. Phys.* **95** 1311–22

Dash J G, Rempel A W and Wettlaufer J S 2006 The physics of premelted ice and its geophysical consequencesy *Rev. Mod. Phys.* **78** 695–741

Denoth A 1999 Wet snow pendular regime: the amount of water in ring-shaped configurations *Cold Regions Sci. Technol.* **30** 13–18

Denoth A 2003 Structural phase changes of the liquid water component in Alpine snow *Cold Regions Sci. Technol.* **37** 227–32

Dominé F, Lauzier T, Cabanes A, Legagneux L, Kuhs W F, Techmer K and Heinrichs T 2003 Snow metamorphism as revealed by scanning electron microscopy *Microsc. Res. Tech.* **62** 33–48

Dominé F and Shepson P B 2002 Air–snow interactions and atmospheric chemistry *Science* **297** 1506–10

Durand G, Gagliardini O, Thorsteinsson T, Svensson A, Kipfstuhl S and Dahl-Jensen D 2006 Ice microstructure and fabric: an up-to-date approach for measuring textures *J. Glaciol.* **52** 619–30

Erbe E F, Rango A, Foster J, Josberger E G, Pooley C and Wergin W P 2003 Collecting, shipping, storing, and imaging snow crystals and ice grains with low–temperature scanning electron mircoscopy *Microsc. Res. Tech.* **62** 19–32

Evans D C B, Nye J F and Cheeseman K J 1976 Kinetic friction of ice *Proc. R. Soc. Lond. Ser. A—Math. Phys. Eng. Sci.* **347** 493–512

Exner H E and Arzt E 1996 Sintering processes *Physical Metallurgy* ed R W Cahn and P Haasen (Amsterdam: Elsevier) pp 2628–62

Fischmeister H F and Arzt E 1983 Densification of powders by particle deformation *Powder Metall.* **26** 82–8

Flin F, Brzoska J B, Lesaffre B, Cileou C and Pieritz R A 2003 Full three–dimensional modelling of curvature–dependent snow metamorphism: first results and comparison with experimental tomographic data *J. Phys. D: Appl. Phys.* **36** A49–54

Flin F, Brzoska J B, Lesaffre B, Coleou C C and Pieritz R A 2004 Three–dimensional geometric measurements of snow microstructural evolution under isothermal conditions *Ann. Glaciol.* **38** 39–44

Freitag J, Wilhelms F and Kipfstuhl S 2004 Microstructure-dependent densification of Polar firn derived from x-ray microtomography *J. Glaciol.* **50** 243–50

Fyffe B and Zaiser M 2004 The effects of snow variability on slab avalanche release *Cold Regions Sci. Technol.* **40** 229–42

German R M 1996 *Sintering Theory and Practice* (New York: Wiley Interscience)

Good W 1987 Thin sections, serial cuts and 3-D analysis of snow *Davos Symp. on Avalanche Formation, Movement and Effects, IAHS Publication* vol 162 (Wallingford, UK) pp 35–47

Gow A J 1968 Deep core studies of the accumulation and densification of snow at Byrd Station and Little America V, Antarctica *Report* 197 (45), US Army Cold Regions Research and Engineering Laboratory

Gow A J 1975 Time–temperature dependence of sintering in perennial isothermal snowpacks *Snow Mechanics* vol 114 (Wallingford, UK: International Association of Hydrological Sciences, IAHS-AISH) pp 25–41

Gubler H 1982 Strength of bonds between ice grains after short contact times *J. Glaciol.* **28** 457–73

Hardy S C 1977 Grain-boundary groove measurement of surface-tension between ice and water *Phil. Mag.* **35** 471–84

Hassold G N, Chen I W and Srolovitz D J 1990 Computer-simulation of final-stage sintering: 1. Model, kinetics, and microstructure *J. Am. Ceram. Soc.* **73** 2857–64

Heierli J and Zaiser M 2006 An analytical model for fracture nucleation in collapsible stratifications *Geophys. Res. Lett.* **33** L06501

Heierli J and Zaiser M 2007 Failure initiation in snow stratifications containing weak layers: Nucleation of whumpfs and slab avalanches *Cold Regions Sci. Technol.* doi:10.1016/j.coldregions.2007.02.007

Hobbs P V 1974 *Ice Physics* (Oxford: Oxford University Press)

Hobbs P V and Mason B J 1964 Sintering and adhesion of ice *Phil. Mag.* **9** 181–97

Hobbs P V and Radke L F 1967 The role of volume diffusion in the metamorphism of snow *J. Glaciol.* **6** 879–91

Iliescu D, Baker I and Cullen D 2002 Preliminary microstructural and microchemical observations on pond and river accretion ice *Cold Regions Sci. Technol.* **35** 81–99

Iliescu D, Baker I and Chang H 2004 Determining the orientations of ice crystals using electron backscatter patterns *Micro. Res. Tech.* **63** 183–7

Jamieson B and Johnston C D 2001 Evaluation of the shear frame test for weak snowpack layers *Ann. Glaciol.* **32** 59–69

Jeffree C E and Read N D 1991 Ambient- and low-temperature scanning electron microscopy *Electron Microscopy of Plant Cells* ed J L Hall and C R Hawes (London: Academic) pp 331–413

Jeffree C E, Read N D, Smith J A C and Dale J E 1987 Water droplets and ice deposits in leaf intercellular spaces—redistribution of water during cryofixation for scanning electron-microscopy *Planta* **172** 20–37

Jellinek H G and Ibrahim S H 1967 Sintering of powdered ice *J. Colloid Interface Sci.* **25** 245–54

Johnson D L 1969 New method of obtaining volume grain-boundary and surface diffusion coefficients from sintering data *J. Appl. Phys.* **40** 192–200

Johnson J B and Schneebeli M 1999 Characterizing the microstructural and micromechanical properties of snow *Cold Regions Sci. Technol.* **30** 91–100

Jones D R H and Chadwick G A 1971 Experimental measurement of solid–liquid interfacial energies—ice–water–sodium chloride system *J. Cryst. Growth* **11** 260–4

Kaempfer T U, Schneebeli M and Sokratov S A 2005 A microstructural approach to model heat transfer in snow *Geophys. Res. Lett.* **32** L21503

Kazaryan A, Wang Y and Patton B R 1999 Generalized phase field approach for computer simulation of sintering: incorporation of rigid–body motion *Scr. Mater.* **41** 487–92

Ketcham W M and Hobbs P V 1969 An experimental determination of surface energies of ice *Phil. Mag.* **19** 1161–73

Kingery W D 1960 Regelation, surface diffusion, and ice sintering *J. Appl. Phys.* **31** 833–8

Kingery W D and Berg M 1955 Study of the initial stages of sintering solids by viscous flow, evaporation-condensation, and self–diffusion *J. Appl. Phys.* **26** 1205–12

Kry P R 1975 Quantitative stereological analysis of grain bonds in snow *J. Glaciol.* **14** 467–77

Kuczynski G C 1949 Self-diffusion in sintering of metallic particles *Trans. Am. Inst. Min. Metall. Eng.* **185** 169–78

Kuroiwa D 1961 A study of ice sintering *Tellus* **13** 252–9

Kuroiwa D 1962 A study of ice sintering *Research Report* 86 US Army Cold Regions Research and Engineering Laboratory

Kuroiwa D 1977 Kinetic friction on snow and ice *J. Glaciol.* **19** 141–52

Legagneux L, Cabanes A and Dominé F 2002 Measurement of the specific surface area of 176 snow samples using methane adsorption at 77 K *J. Geophys. Res.—Atmos.* **107** 4335

Legagneux L and Dominé F 2005 A mean field model of the decrease of the specific surface area of dry snow during isothermal metamorphism *J. Geophys. Res.—Earth Surf.* **110** F04011

Legagneux L, Lauzier T, Dominé F, Kuhs W F, Heinrichs T and Techmer K 2003 Rate of decay of specific surface area of snow during isothermal experiments and morphological changes studied by scanning electron microscopy *Can. J. Phys.* **81** 459–68

Legagneux L, Taillandier A S and Dominé 2004 Grain growth theories and the isothermal evolution of the specific surface area of snow *J. Appl. Phys.* **95** 6175–84

Legrand M and Mayewski P 1997 Glaciochemistry of Polar ice cores: a review *Rev. Geophys.* **35** 219–43

Lehning M, Bartelt P, Brown B, Fierz C and Satyawali P 2002 A physical SNOWTACK model for the Swiss avalanche warning: II. Snow microstructure *Cold Regions Sci. Technol.* **35** 147–67

Lenel F V 1948 Sintering in the presence of a liquid phase *Trans. Am. Inst. Mining Metall. Eng.* **175** 878–905

Libbrecht K G 2005 The physics of snow crystals *Rep. Prog. Phys.* **68** 855–95

Liu J, Lal A and German R M 1999 Densification and shape retention in supersolidus liquid phase sintering *Acta Mater.* **47** 4615–26

Liu J Z and Fang Z G Z 2004 Quantitative characterization of microstructures of liquid-phase-sintered two–phase materials *Metall. Mater. Trans. A—Phys. Metall. Mater. Sci.* A **35** 1881–8

Liu J X and German R M 2001 Microstructure effect on dihedral angle in liquid-phase sintering *Metall. Mater. Trans. A—Phys. Metall. Mater. Sci.* **32** 165–9

Lu P Z, Xu X P, Yi W W and German R M 2001 Porosity effect on densification and shape distortion in liquid phase sintering *Mater. Sci. Eng. A—Struct. Mater. Prop. Microstruct. Process.* **318** 111–21

Lundy C C, Edens M Q and Brown R L 2002 Measurement of snow density and microstructure using computed tomography *J. Glaciol.* **48** 312–16

Mader H M 1992a Observations of the water–vein system in polycrystalline ice *J. Glaciol.* **38** 333–47

Mader H M 1992b The thermal–behavior of the water–vein system in polycrystalline ice *J. Glaciol.* **38** 359–74

Maeno N and Arakawa M 2004 Adhesion shear theory of ice friction at low sliding velocities, combined with ice sintering *J. Appl. Phys.* **95** 134–9

Maeno N and Ebinuma T 1983 Pressure sintering of ice and its implication to the densification of snow at Polar glaciers and ice sheets *J. Phys. Chem.* **87** 4103–10

Marbouty D 1980 An experimental-study of temperature-gradient metamorphism *J. Glaciol.* **26** 303–12

Marmo B A, Blackford J R and Jeffree C E 2005 Ice friction, wear features and their dependence on sliding velocity and temperature *J. Glaciol.* **51** 391–8

Maupetit F and Delmas R J 1994 Snow chemistry of high-altitude glaciers in the French Alps *Tellus Ser. B—Chem. Phys. Meteorol.* **46** 304–24

Miller D A, Adams E E and Brown R L 2003 A microstructural approach to predict dry snow metamorphism in generalized thermal conditions *Cold Regions Sci. Technol.* **37** 213–26

Min D H and Wong H 2006 The effect of strong surface energy anisotropy on migrating grain–boundary grooves *J. Appl. Phys.* **100** 053523

Mullins W W 1957 Theory of thermal grooving *J. Appl. Phys.* **28** 333–9

Mulvaney R, Wolff E W and Oates K 1988 Sulfuric-acid at grain-boundaries in Antarctic ice *Nature* **331** 247–9

Nickus U *et al* 1997 SNOSP: Ion deposition and concentration in high Alpine snow packs *Tellus Ser. B—Chem. Phys. Meteorol.* **49** 56–71

Nye J F 1989 The geometry of water veins and nodes in polycrystalline ice *J. Glaciol.* **35** 17–22

Obbard R, Baker I and Sieg K 2006 Using electron backscatter diffraction patterns to examine recrystallization in Polar ice sheets *J. Glaciol.* **52** 546–57

Obbard R, Iliescu D, Cullen D, Chang J and Baker I 2003 SEM/EDS comparison of Polar and seasonal temperate ice *Microsc. Res. Tech.* **62** 49–61

Offenbacher E L, Roselman I C and Tabor D 1973 *Physics and Chemistry of Ice* ed E Whalley, S J Jones and W Gold (Ottawa: Royal Society of Canada) pp 337–81

Olevsky E A, Tikare V and Garino T 2006 Multi-scale study of sintering: A review *J. Am. Ceram. Soc.* **89** 1914–22

Pan J Z 2003 Modelling sintering at different length scales *Int. Mater. Rev.* **48** 69–85

Pan J and Cocks A C F 1995 A numerical technique for the analysis of coupled surface and grain–boundary diffusion *Acta Metall. Mater.* **43** 1395–406

Pan J, Le H, Kucherenko S and Yeomans J A 1998 A model for the sintering of spherical particles of different sizes by solid state diffusion *Acta Mater.* **46** 4671–90

Parhami F, McMeeking R M, Cocks A C F and Suo Z 1999 A model for the sintering and coarsening of rows of spherical particles *Mech. Mater.* **31** 43–61

Perla R 1982 Preparation of section planes in snow specimens *J. Glaciol.* **28** 199–204

Petrenko V 1994 The surface of ice *Report* 94-22 US Army Cold Regions Research and Engineering Laboratory

Petrenko V and Whitworth R W 2002 *Physics of Ice* (Oxford, UK: Oxford University Press)

Pielmeier C and Schneebeli M 2003 Developments in the stratigraphy of snow *Surv. Geophys.* **24** 389–416

Ramseier R and Keeler C M 1966 The sintering process in snow *J. Glaciol.* **6** 421–4

Rango A, Wergin W P and Erbe E F 1996a Snow crystal imaging using scanning electron microscopy: 1. Precipitated snow *Hydrol. Sci. J.—J. Sci. Hydrol.* **41** 219–33

Rango A, Wergin W P and Erbe E F 1996b Snow crystal imaging using scanning electron microscopy: 2. Metamorphosed snow *Hydrol. Sci. J.—J. Sci. Hydrol.* **41** 235–50

Rango A, Wergin W P, Erbe E F and Josberger E G 2000 Snow crystal imaging using scanning electron microscopy: 3. Glacier ice, snow and biota *Hydrol. Sci. J.—J. Sci. Hydrol.* **45** 357–75

Raymond C F and Tusima K 1979 Grain coarsening of water–saturated snow *J. Glaciol.* **22** 83–105

Read N D and Jeffree C E 1991 Low-temperature scanning electron-microscopy in biology *J. Microsc.—Oxford* **161** 59–72

Riedel H, Zipse H and Svoboda J 1994 Equilibrium pore surfaces, sintering stresses and constitutive-equations for the intermediate and late stages of sintering: 2. Diffusional densification and creep *Acta Metall. Mater.* **42** 445–52

Rosenthal W, Saleta J and Dozier J 2007 Scanning electron microscopy of impurity structures in snow *Cold Regions Sci. Technol.* **47** 80–9

Satyawali P K, Sinha N K and Sethi D N 2003 Double-microtoming technique for snow studies *Can. J. Phys.* **81** 529–37

Saylor D M and Rohrer G S 1999 Measuring the influence of grain–boundary misorientation on thermal groove geometry in ceramic polycrystals *J. Am. Ceram. Soc.* **82** 1529–36

Schneebeli M, Pielmeier C and Johnson J B 1999 Measuring snow microstructure and hardness using a high resolution penetrometer *Cold Regions Sci. Technol.* **30** 101–14

Schneebeli M and Sokratov S A 2004 Tomography of temperature gradient metamorphism of snow and associated changes in heat conductivity *Hydrol. Process.* **18** 3655–65

Schulson E M 1999 The structure and mechanical behavior of ice *J. Mat.—J. Min. Met. Mater. Soc.* **51** 21–7

Schweizer J, Jamieson J B and Schneebeli M 2003 Snow avalanche formation *Rev. Geophys.* **41** 1016

Schweizer J, Schneebeli M, Fierz C and Fohn P M B 1995 Snow mechanics and avalanche formation—field experiments on the dynamic-response of the snow cover *Surv. Geophys.* **16** 621–33

Shapiro L H, Johnson J B, Sturm M and Blaisdell G L 1997 Snow mechanics: review of the state of knowledge and applications *Report 97-3* US Army Cold Regions Research and Engineering Laboratory

Sinha N K 1977 Technique for studying structure of sea ice *J. Glaciol.* **18** 315–23

Smith C S 1948 Grains, phases, and interfaces—an interpretation of microstructure *Trans. Am. Inst. Min. Metall. Eng.* **175** 15–51

Sturm M and Benson C S 1997 Vapor transport, grain growth and depth–hoar development in the subarctic snow *J. Glaciol.* **43** 42–59

Sun B and Suo Z 1997 A finite element method for simulating interface motion2 Large shape change due to surface diffusion *Acta Mater.* **45** 4953–62

Sun B, Suo Z and Yang W 1997 A finite element method for simulating interface motion: 1. Migration of phase and grain boundaries *Acta Mater.* **45** 1907–15

Svoboda J and Riedel H 1992 Pore–boundary interactions and evolution-equations for the porosity and the grain-size during sintering *Acta Metall. Mater.* **40** 2829–40

Svoboda J and Riedel H 1995 New solutions describing the formation of interparticle necks in solid-state sintering *Acta Metall. Mater.* **43** 1–10

Svoboda J, Riedel H and Zipse H 1994 Equilibrium pore surfaces, sintering stresses and constitutive-equations for the intermediate and late stages of sintering: 1. Computation of equilibrium surfaces *Acta Metall. Mater.* **42** 435–43

Swinkels F B and Ashby M F 1981 Overview 11—A 2nd report on sintering diagrams *Acta Metall.* **29** 259–81

Swinkels F B, Wilkinson D S, Arzt E and Ashby M F 1983 Mechanisms of hot–isostatic pressing *Acta Metall.* **31** 1829–40

Tusima K 1977 Friction of a steel ball on a single crystal of ice *J. Glaciol.* **19** 225–35

Tusima K 1985 Grain coarsening of snow particles immersed in water and solutions *Ann. Glaciol.* **6** 126–9

Wakai F 2006 Modeling and simulation of elementary processes in ideal sintering *J. Am. Ceram. Soc.* **89** 1471–84

Wakai F, Yoshida M, Shinoda Y and Akatsu T 2005 Coarsening and grain growth in sintering of two particles of different sizes *Acta Mater.* **53** 1361–71

Walford M E R and Nye J F 1991 Measuring the dihedral angle of water at a grain-boundary in ice by an optical diffraction method *J. Glaciol.* **37** 107–12

Walford M E R, Roberts D W and Hill I 1987 Optical measurements of water lenses in ice *J. Glaciol.* **33** 159–61

Wang Y U 2006 Computer modeling and simulation of solid-state sintering: a phase field approach *Acta Mater.* **54** 953–61

Wang Y Z, Liu Y H, Ciobanu C and Patton B R 2000 Simulating microstructural evolution and electrical transport in ceramic gas sensors *J. Am. Ceram. Soc.* **83** 2219–26

Weeks W F and Ackley S F 1982 The growth, structure, and properties of sea ice *Report* 82–1 US Army Cold Regions Research and Engineering Laboratory

Weeks W F and Ackley S F 1986 The growth, structure and properties of sea ice *The Geophysics of Sea Ice* ed N Untersteiner (*NATO ASI Series, Series B, Physics* vol 146) (New York: Plenum)

Wergin W P, Rango A and Erbe E F 1995 Observations of snow crystals using low-temperature scanning electron-microscopy *Scanning* **17** 41–50

Wergin W P, Rango A and Erbe E F 1998 Image comparisons of snow and ice crystals photographed by light (video)

microscopy and low-temperature scanning electron microscopy *Scanning* **20** 285–96

Wergin W P, Rango A, Foster J, Erbe E F and Pooley C 2002 Irregular snow crystals: structural features as revealed by low temperature scanning electron microscopy *Scanning* **24** 247–56

Wettlaufer J S 1999 Ice surfaces: macroscopic effects of microscopic structure *Phil. Trans. R. Soc. Lond. Ser. A—Math. Phys. Eng. Sci.* **357** 3403–25

Wettlaufer J S 2001 Dynamics of ice surfaces *Interface Sci.* **9** 117–29

Wilen L A and Dash J G 1995 Giant facets at ice grain–boundary grooves *Science* **270** 1184–6

Wilen L A, Diprinzio C L, Alley R B and Azuma N 2003 Development, principles, and applications of automated ice fabric analyzers *Microsc. Res. Tech.* **62** 2–18

Wilkinson D S 1988 A pressure-sintering model for the densification of Polar firn and glacier ice *J. Glaciol.* **34** 40–5

Wilkinson D S and Ashby M F 1975 Pressure sintering by power law creep *Acta Metall.* **23** 1277–85

Williamson A M, Lips A, Clark A and Hall D 1999 Late stage coarsening in concentrated ice systems *Faraday Discuss.* **112** 31–49

Wolff E W and Reid A P 1994 Capture and scanning electron-microscopy of individual snow crystals *J. Glaciol.* **40** 195–7

Xin T H and Wong H 2003 Grain-boundary grooving by surface diffusion with strong surface energy anisotropy *Acta Mater.* **51** 2305–17

Zhang W and Gladwell I 2005 Thermal grain boundary grooving with anisotropic surface free energy in three dimensions *J. Cryst. Growth* **277** 608–22

Zhang W, Sachenko P and Gladwell I 2004 Thermal grain boundary grooving with anisotropic surface free energies *Acta Mater.* **52** 107–16

Zhang W, Sachenko P and Schneibel J H 2002 Kinetics of thermal grain boundary grooving for changing dihedral angles *J. Mater. Res.* **17** 1495–501

Zhang W and Schneibel J H 1995 The sintering of 2 particles by surface and grain-boundary diffusion—a 2-dimensional numerical study *Acta Metall. Mater.* **43** 4377–86